

Unitary Coupled Cluster: Seizing the Quantum Moment

Ilias Magoulas* and Francesco A. Evangelista*

Department of Chemistry and Cherry Emerson Center for Scientific Computation, Emory University, Atlanta, Georgia 30322, USA

E-mail: ilias.magoulas@emory.edu; francesco.evangelista@emory.edu

Abstract

Shallow, CNOT-efficient quantum circuits are crucial for performing accurate computational chemistry simulations on current noisy quantum hardware. Here, we explore the usefulness of non-iterative energy corrections, based on the method of moments of coupled-cluster theory, for accelerating convergence toward full configuration interaction. Our preliminary numerical results relying on iteratively constructed ansätze suggest that chemically accurate energies can be obtained with substantially more compact circuits, implying enhanced resilience to gate and decoherence noise.

The first electronic structure calculation on quantum hardware was reported more than 10 years ago.¹ It involved the iterative quantum phase estimation computation of the spectrum of H_2 in a minimum basis set. Since then, in tandem with various technological innovations, significant algorithmic advances have taken place aimed at the full utilization of the current generation of noisy intermediate-scale quantum devices.² Of particular importance is the arsenal of hybrid quantum-classical approaches,^{3,4} including the variational (VQE),^{5–9} contracted,¹⁰ and projective¹¹ (PQE) quantum eigensolvers, quantum imaginary time evolution,^{12,13} and quantum subspace diagonalization techniques,^{12,14–17} to mention a few. Such schemes require much shallower circuits than pure quantum algorithms, e.g., quantum phase estimation,^{18–20} substantially reducing the computational cost and sensitivity to gate and decoherence noise.

To pave the way toward practical and robust computations on actual quantum devices, various schemes have been devised to reduce the circuit depth of hybrid quantum-classical algorithms even further. In the case of ansatz-dependent approaches, which are of particular importance to this work, the construction of compact, yet suffi-

ciently expressive, trial states is crucial. In general, the trial state is expressed as

$$|\Psi^{(T)}(\mathbf{t})\rangle = U^{(T)}(\mathbf{t}) |\Phi\rangle, \quad (1)$$

where $\mathbf{t} = (t_1, t_2, \dots)$ is a vector of parameters, $|\Phi\rangle$ is a reference state that can be easily realized on the quantum device, and

$$U^{(T)}(\mathbf{t}) = \prod_{\mu} U_{\mu}^{(T)}(t_{\mu}) \quad (2)$$

is the unitary operator that rotates $|\Phi\rangle$ to the trial state $|\Psi^{(T)}(\mathbf{t})\rangle$. Equation (2) immediately reveals two complementary strategies for reducing the circuit complexity of ansatz-dependent algorithms. First, it is beneficial to minimize the number of parameters entering $U^{(T)}$, without, however, significantly sacrificing the expressivity of the ansatz. It is, thus, not surprising that fixed ansätze have been almost invariably replaced by their iteratively constructed counterparts.^{10,11,21–27} In doing so, one eliminates the typically large number of superfluous parameters inadvertently incorporated in fixed-ansätze approaches. Second, the form of the individual unitaries $U_{\mu}^{(T)}$ should be such that the corresponding quantum circuits are as compact as possible. To that end, different flavors of ansätze have been explored, typically derived from the unitary extension^{28–40} of coupled-cluster theory^{41–46} (UCC). In this case, the $U_{\mu}^{(T)}(t_{\mu})$ unitaries have the form

$$U_{\mu}^{(T)}(t_{\mu}) = e^{t_{\mu} \kappa_{\mu}}, \quad (3)$$

where κ_{μ} is a generic fermionic anti-Hermitian operator. In the language of second quantization and in the case of an n -body operator, κ_{μ} is defined as

$$\kappa_{\mu} \equiv \kappa_{i_1 \dots i_n}^{a_1 \dots a_n} = a^{a_1} \dots a^{a_n} a_{i_n} \dots a_{i_1} - a^{i_1} \dots a^{i_n} a_{a_n} \dots a_{a_1}, \quad (4)$$

where a_p ($a^p \equiv a_p^\dagger$) is the annihilation (creation) operator acting on spinorbital ϕ_p and indices i_1, i_2, \dots or i, j, \dots (a_1, a_2, \dots or a, b, \dots) label spinorbitals occupied (unoccupied) in $|\Phi\rangle$. Although starting from a fermionic UCC unitary and translating it to the qubit space is a natural choice for the study of electronic structure problems, it generally leads to circuits containing a substantial number of CNOT gates. This is particularly problematic, since current hardware implementations of two-qubit gates, such as CNOTs, are typically ~ 10 times noisier than their one-qubit analogs. More CNOT-efficient ansätze are obtained, for example, by directly building UCC in the qubit space^{22,24,47} or employing the fermionic-excitation-based (FEB) circuits and their qubit (QEB) counterparts.^{23,25,26,48–50} Approximate implementations of the FEB and QEB circuits have recently been explored, resulting in single- and two-qubit gate counts that scale linearly with the excitation rank.⁵¹

Another promising approach for reducing quantum resource requirements that has received relatively little attention, is the use of non-iterative energy corrections. Such schemes, in conjunction with iteratively constructed ansätze, have the potential to accelerate convergence toward the exact, full configuration interaction (FCI), solution, thus decreasing the depth of the underlying quantum circuits. This avenue was initially explored in the context of the iterative qubit coupled cluster (iQCC) approach²⁴ by Ryabinkin et al.⁵² By considering various low-order perturbative corrections to the iQCC energies, they were able to achieve a given level of accuracy with a smaller number of iQCC iterations.

Similar in spirit to the work of Ryabinkin et al., in this study we explore the usefulness of non-iterative energy corrections resulting from the formalism of the method of moments of CC (MMCC) equations^{53–66} in accelerating the convergence to FCI of adaptive schemes. Corrections based on the MMCC framework have several desirable properties. Unlike non-iterative corrections based on many-body perturbation theory arguments,^{67–76} which generally fail when non-dynamical correlations become substantial, MMCC-type corrections are robust in the presence of quasi-degeneracies encountered in typical problems of chemical interest, such as single bond breaking and biradicals. In its exact form, the MMCC framework provides the non-iterative correction to the energy

of an approximate CC method needed to recover the FCI energy. Although in practice one computes an approximate MMCC correction, improving its quality by incorporating higher-rank moments is straightforward, albeit computationally demanding on a classical machine. Nevertheless, in the case of a unitary ansatz, the necessary ingredients to compute such corrections can be efficiently calculated on a quantum computer (vide infra). Furthermore, UCC-based approaches provide upper bounds to the FCI energy, rendering them immune to the catastrophic failures plaguing traditional single-reference CC methods in the presence of strong correlations, and excellent starting points for non-iterative corrections (see, also, ref 57 for the generalization of the MMCC formalism to extended coupled cluster theory). MMCC methods have been recently introduced to the realm of quantum computing, albeit from a different perspective. Peng and Kowalski have constructed a compact representation of non-unitary operators on quantum devices.⁷⁷ This allowed them to devise quantum algorithms for computing MMCC corrections to conventional, i.e., non-unitary, CC schemes. Although Peng and Kowalski also outline how to extend the MMCC formalism to UCC ansätze in a way similar to our approach, to the best of our knowledge the corresponding algorithm has never been implemented.

We begin our discussion of non-iterative corrections by first summarizing the salient features of the quantum algorithms used to optimize the trial state. We employed the adaptive derivative-assembled pseudo-Trotterized VQE (ADAPT-VQE)²¹ and selected PQE (SPQE)¹¹ approaches, which are based on iteratively constructed ansätze optimized with VQE and PQE, respectively. Recall that in the VQE and PQE schemes, the energy $E^{(T)}$ is computed as the expectation value of the Hamiltonian with respect to the trial state,

$$E^{(T)} = \langle \Psi^{(T)} | H | \Psi^{(T)} \rangle = \langle \Phi | \bar{H}^{(T)} | \Phi \rangle, \quad (5)$$

where $\bar{H}^{(T)} = U^{(T)\dagger} H U^{(T)}$ is the similarity-transformed Hamiltonian. Thus, both VQE and PQE provide upper bounds to the FCI energy. At a high level, both algorithms rely on essentially the same two alternating steps. First, there is an expansion step promoting the growth of the ansatz. This is accomplished by ordering the operators in a given operator pool based on a predefined im-

portance criterion and adding the most important operator(s) to the ansatz. In the case of VQE, the energy gradients

$$g_\mu(T) \equiv \frac{\partial E^{(T)}}{\partial t_\mu} \quad (6)$$

play the role of the importance criterion, while in PQE the residuals of the UCC equations are used instead. Recall that the UCC residuals are projections onto the manifold of excited Slater determinants ($|\Phi_\mu\rangle \equiv \kappa_\mu |\Phi\rangle$) of the connected cluster form of the Schrödinger equation with the UCC ansatz, eq (1),

$$r_\mu(T) \equiv \langle \Phi_\mu | \bar{H}^{(T)} | \Phi \rangle. \quad (7)$$

Note that, as shown in ref 11, the residuals of all operators in the pool can be efficiently estimated by repeated measurements of the “residual state,” defined as

$$|\tilde{r}(T)\rangle = U^{(T)\dagger} e^{i\Delta t H} U^{(T)} |\Phi\rangle. \quad (8)$$

The second step of the algorithm is the optimization of the ansatz parameters. If we partition the full operator space into those incorporated in the ansatz (P) and those excluded (Q), then for VQE the optimization is performed variationally, which translates into enforcing the condition $g_p = 0 \forall \kappa_p \in P$. In the PQE case, a similar condition is imposed, this time, however, for the residuals ($r_p = 0 \forall \kappa_p \in P$). As shown in ref 11, the exact evaluation of a residual element in PQE has the same cost as the exact estimation of the corresponding gradient element in VQE using the parameter shift rule.^{78,79} The remaining details of the SPQE and ADAPT-VQE algorithms can be found in refs 11 and 21, respectively.

Next, we move on with the discussion of the non-iterative corrections. Here, we consider two families of non-iterative MMCC-type corrections. The first one has the form

$$\delta_{\text{Ia}}(T) = \sum_\mu \frac{|r_\mu(T)|^2}{E^{(T)} - E_\mu^{(T)}}, \quad (9)$$

where $r_\mu(T)$ are the residuals or moments of the UCC equations^{53,54,80} and $E_\mu^{(T)} = \langle \Phi_\mu | \bar{H}^{(T)} | \Phi_\mu \rangle$ the diagonal elements of $\bar{H}^{(T)}$. Note that the summation over μ excludes the reference determinant. Equation (9) can be regarded as the direct translation of biorthogonal MMCC expansions^{59–61} and their CC($P;Q$) generalization^{66,81,82}

to the language of UCC. In the numerator of the CC($P;Q$) correction appears the product of moments of CC equations corresponding to the right and left CC states. Recall that traditional CC theory is non-Hermitian and as such the CC similarity-transformed Hamiltonian has distinct right and left eigenvectors. Since the UCC similarity-transformed Hamiltonian is Hermitian, in the translation process, the left-state moment is replaced by the complex conjugate of the right moment. From an alternative point of view, eq (9) can be derived using Löwdin’s partitioning procedure taking the zeroth-order part of the Hamiltonian to be the diagonal elements of $\bar{H}^{(T)}$.⁸³

In our current implementation, the summation appearing in eq (9) is performed over all excited Slater determinants $|\Phi_\mu\rangle$ for which $r_\mu(T) \neq 0$, namely, $|\Phi_\mu\rangle \in Q$ for PQE and $|\Phi_\mu\rangle \in P \oplus Q$ in the case of VQE. For example, in a UCCSD calculation relying on PQE optimization (UCCSD-PQE), the optimum parameters are obtained by imposing the residual conditions

$$r_a^i(\text{UCCSD-PQE}) \equiv \langle \Phi_i^a | \bar{H}^{(\text{UCCSD-PQE})} | \Phi \rangle = 0 \quad (10)$$

and

$$r_{ab}^{ij}(\text{UCCSD-PQE}) \equiv \langle \Phi_{ij}^{ab} | \bar{H}^{(\text{UCCSD-PQE})} | \Phi \rangle = 0. \quad (11)$$

Thus, the summation in eq (9) defining the $\delta_{\text{Ia}}(\text{UCCSD-PQE})$ moment correction runs over all triply, quadruply, etc. excited Slater determinants (note that, unlike the case of traditional CCSD where the moment expansion naturally terminates after hexuples, for UCCSD-PQE all moments corresponding to higher-than-double excitations are, in principle, non-zero). Alternatively, in a VQE-based UCCSD (UCCSD-VQE) computation, the parameter optimization is performed variationally, i.e., by enforcing

$$g_a^i \equiv \frac{\partial E^{(\text{UCCSD-VQE})}}{\partial t_a^i} = 0 \quad (12)$$

and

$$g_{ab}^{ij} \equiv \frac{\partial E^{(\text{UCCSD-VQE})}}{\partial t_{ab}^{ij}} = 0. \quad (13)$$

Consequently, since no residual condition is imposed, the $\delta_{\text{Ia}}(\text{UCCSD-VQE})$ non-iterative correction involves all UCCSD-VQE moments, including those corresponding to singles and doubles. In this case, the appropriate schemes are based on the gen-

eralized MMCC formalism that was introduced in the context of extended coupled cluster theory.⁵⁷

Next, we consider the computational burden associated with the evaluation of eq (9). To this end, we examine the availability of its constituents. In the case of SPQE, the $r_\mu(\text{SPQE})$ residuals are already available, since they are generated for the selection of new operators. This is analogous to how perturbative energy corrections are evaluated in selected configuration interaction (CI) techniques, such as the CI method using perturbative selection made iteratively,^{84–86} adaptive CI,^{87,88} and adaptive sampling CI,⁸⁹ to mention a few. In the case of ADAPT-VQE simulations, the residuals need to be evaluated, but this can be efficiently accomplished by repeated measurements of the residual vector, as discussed above. Furthermore, both SPQE and ADAPT-VQE have access to the $E^{(T)}$ energy of the trial state, as part of the parameter optimization process. Thus, the major computational overhead is the evaluation of the diagonal elements of the similarity-transformed Hamiltonian in every macro-iteration. To reduce the computational cost associated with the evaluation of $E_\mu^{(T)}$, we also consider two approximations to the denominators that enter into eq (9). In the first one, denoted as $\delta_{\text{Ib}}(T)$, we replace the similarity-transformed Hamiltonian in $E_\mu^{(T)}$ by the bare Hamiltonian,

$$\delta_{\text{Ib}}(T) = \sum_{\mu} \frac{|r_{\mu}(T)|^2}{E^{(T)} - E_{\mu}}. \quad (14)$$

This allows us to efficiently evaluate the $E_{\mu} = \langle \Phi_{\mu} | H | \Phi_{\mu} \rangle$ energies only once per simulation using a classical algorithm. The second approximation, designated as $\delta_{\text{Ic}}(T)$, is more drastic, replacing the entire denominator appearing in eq (9) by its Møller–Plesset counterpart,

$$\delta_{\text{Ic}}(T) = \sum_{\mu} \frac{|r_{\mu}(T)|^2}{\Delta_{\mu}}, \quad (15)$$

where $\Delta_{\mu} \equiv \Delta_{i_1 \dots i_n}^{a_1 \dots a_n} = \epsilon_{i_1} + \dots + \epsilon_{i_n} - \epsilon_{a_1} - \epsilon_{a_n}$ with ϵ_p denoting the Hartree–Fock energy of spinorbital ϕ_p . Note that unlike eqs (9) and (15), the approximation defined in eq (14) is not rigorously size consistent [see the Supporting Information for the proof and underlying conditions for the size consistency of eqs (9) and (15)]. Nevertheless, our preliminary numerical results suggest that this is not a major issue (vide infra).

The second family of non-iterative corrections we

consider is based on the one defining the original renormalized and completely renormalized CC approaches,^{53–55} namely,

$$\delta_{\text{II}}(T) = \sum_{\mu} \frac{\langle \Psi^{(\text{ext})} | U^{(T)} | \Phi_{\mu} \rangle r_{\mu}(T)}{\langle \Psi^{(\text{ext})} | \Psi^{(T)} \rangle}. \quad (16)$$

In eq (16), $|\Psi^{(\text{ext})}\rangle$ is the wavefunction from an external source and serves as an approximation to the FCI wavefunction. If $|\Psi^{(\text{ext})}\rangle \equiv |\Psi^{(\text{FCI})}\rangle$, then eq (16) yields the exact MMCC correction, i.e., $E^{(T)} + \delta_{\text{II}}(T) = E^{(\text{FCI})}$. In this regard, eq (16) shares the same philosophy with externally corrected CC approaches.^{90–102} The derivation of this non-iterative correction can be found in the Appendix of Peng and Kowalski.⁷⁷ As was the case with eqs (9), (14), and (15), the summation appearing in eq (16) involves all excited Slater determinants $|\Phi_{\mu}\rangle$ for which $r_{\mu}(T) \neq 0$. An intriguing aspect of this non-iterative correction is its flexibility regarding the external state. One has the possibility of utilizing any quantum algorithm that can produce an approximate eigenstate of the Hamiltonian and combining it with any ansatz-dependent scheme with the intention of improving the results of both.

To assess the ability of the non-iterative, MMCC-type, energy corrections explored in this study to accelerate convergence toward FCI and reduce the resources used by the underlying quantum algorithms, we performed numerical simulations of the symmetric dissociation of the H_6 linear chain, as described by the minimum STO-6G basis.¹⁰³ In these preliminary calculations, we considered three representative points along the potential energy curve, characterized by the distances between neighboring H atoms of $R_{\text{H-H}} = 1.0, 2.0, \text{ and } 3.0 \text{ \AA}$, corresponding to the equilibrium, recoupling, and strongly correlated regions of the potential, respectively. The underlying quantum algorithms used to gauge the performance of the $\delta_{\text{I}}(T)$ corrections, eqs (9), (14), and (15), were SPQE and ADAPT-VQE. To further reduce the depth of the resulting circuits, we employed the CNOT-efficient FEB-SPQE (fermionic operators) and QEB-ADAPT-VQE (qubit operators) variants. In the case of SPQE, we also considered the approximate FEB scheme (aFEB), which has been shown to faithfully reproduce the parent FEB-SPQE energetics with negligible symmetry breaking and a linear CNOT count.⁵¹ In benchmarking the $\delta_{\text{II}}(T)$ correction, the trial state was obtained with VQE

using a UCCSD ansatz. As a proof of principle, the external states were initially taken to be UCCGSD and UCCSDTQPH, optimized with VQE and PQE, respectively. Both UCCGSD and UCCSDTQPH are exact in the case of H_6 /STO-6G and the δ_{II} (UCCSD) correction to the UCCSD energies reproduced the FCI result with microhartree or better accuracy. In the production run, the external states were those extracted at every macro-iteration of QEB-ADAPT-VQE simulations. This approach shares the same philosophy with the externally corrected CCSD methods based on FCI quantum Monte Carlo¹⁰⁰ and selected CI wavefunctions^{101,102} (see, also, the semi-stochastic CC(P ; Q) scheme based on FCI quantum Monte Carlo¹⁰⁴ and its selected CI counterpart¹⁰⁵).

All SPQE simulations employed a full operator pool and macro-iteration threshold of $10^{-2} E_h$. The PQE micro-iteration threshold was set to $10^{-5} E_h$ while the direct inversion of the iterative subspace^{106–108} was utilized to accelerate convergence. Although in typical SPQE runs, multiple operators are added to the ansatz per macro-iteration, here we followed the ADAPT-VQE paradigm and added operators sequentially. This allowed us to properly examine the ability of the non-iterative corrections to accelerate convergence of SPQE toward FCI. The ADAPT-VQE simulations relied on a pool of generalized singles and doubles^{109,110} and macro- and micro-iteration thresholds of $10^{-3} E_h$ and $10^{-5} E_h$, respectively. The non-iterative energy corrections explored in this study have been implemented in a local version of QForte.¹¹¹ All computations employed restricted Hartree–Fock references, with the one- and two-electron integrals obtained from Psi4.¹¹²

We begin the discussion of our numerical results by examining the ability of the non-iterative, MMCC-type, energy corrections defined in eqs (9), (14), and (15) to accelerate the convergence of FEB-SPQE simulations toward FCI. To that end, in the top panels to Figure 1 we compare the energies resulting from FEB-SPQE and FEB-SPQE $_{I_x} \equiv \text{FEB-SPQE} + \delta_{I_x}$, with $x = a, b, c$. A quick inspection of Figure 1 immediately reveals that all three corrections are capable of reproducing the FCI data within the chemical accuracy of $1 mE_h$ more rapidly than the underlying FEB-SPQE approach. Their performance is particularly impressive in the weakly and moderately correlated regions, requiring as much as $\sim 45\%$ and $\sim 20\%$ fewer parameters than FEB-SPQE. This emphasizes the

exceptional ability of such non-iterative corrections to recover dynamical correlation effects. The decrease in the number of parameters is accompanied by similarly remarkable reductions in the CNOT counts of the corresponding ansatz circuits, as illustrated in the bottom panels to Figure 1. In comparing the various non-iterative corrections among themselves, the FEB-SPQE $_{I_c}$ scheme that relies on the standard Møller–Plesset denominator has the least favorable performance. With the exception of the very early stages of the FEB-SPQE simulations, FEB-SPQE $_{I_b}$ faithfully reproduces the results of its FEB-SPQE $_{I_a}$ parent. This remains true even near the dissociation threshold of H_6 , represented by the geometry characterized by $R_{H-H} = 3.0 \text{ \AA}$. This implies that the size inconsistency introduced in the denominator of eq (14) is not severe, at least in the case of H_6 . As a result, in the subsequent benchmarks we will be focusing on the δ_{I_b} correction, since it not only provides results similar to the more complete δ_{I_a} scheme, but is also more computationally efficient (vide supra).

In an effort to reduce the circuit depth even further, we combine the δ_{I_b} non-iterative correction with aFEB-SPQE. As already mentioned above, the recently introduced aFEB circuits are approximate implementations of the CNOT-efficient FEB ones that require a number of CNOT gates that scales linearly with the excitation rank of a given operator.⁵¹ Furthermore, although the aFEB approximation breaks the particle number N and total spin projection S_z symmetries, it has been demonstrated that aFEB-SPQE is characterized by an essentially negligible symmetry contamination and a faithful reproduction of the parent FEB-SPQE energetics. As might have been anticipated, the same is true when we examine the energies resulting from their δ_{I_b} -corrected counterparts. Indeed, as shown in Figure S1 of the Supporting Information, the aFEB-SPQE $_{I_b}$ data is practically indistinguishable from those obtained with FEB-SPQE $_{I_b}$. This is even true in the recoupling region, characterized by $R_{H-H} = 2.0 \text{ \AA}$, where the largest deviation, on the order of $0.1 mE_h$, is observed. At this point, it is worth mentioning that due to the symmetry breaking introduced by the aFEB quantum circuits, aFEB-SPQE has non-zero moments corresponding to Slater determinants with $N \neq 6$ and/or $S_z \neq 0$ for the ground electronic state of H_6 . In principle, one could incorporate such Fock-space moments into the MMCC-type non-iterative corrections to improve the quality of the results

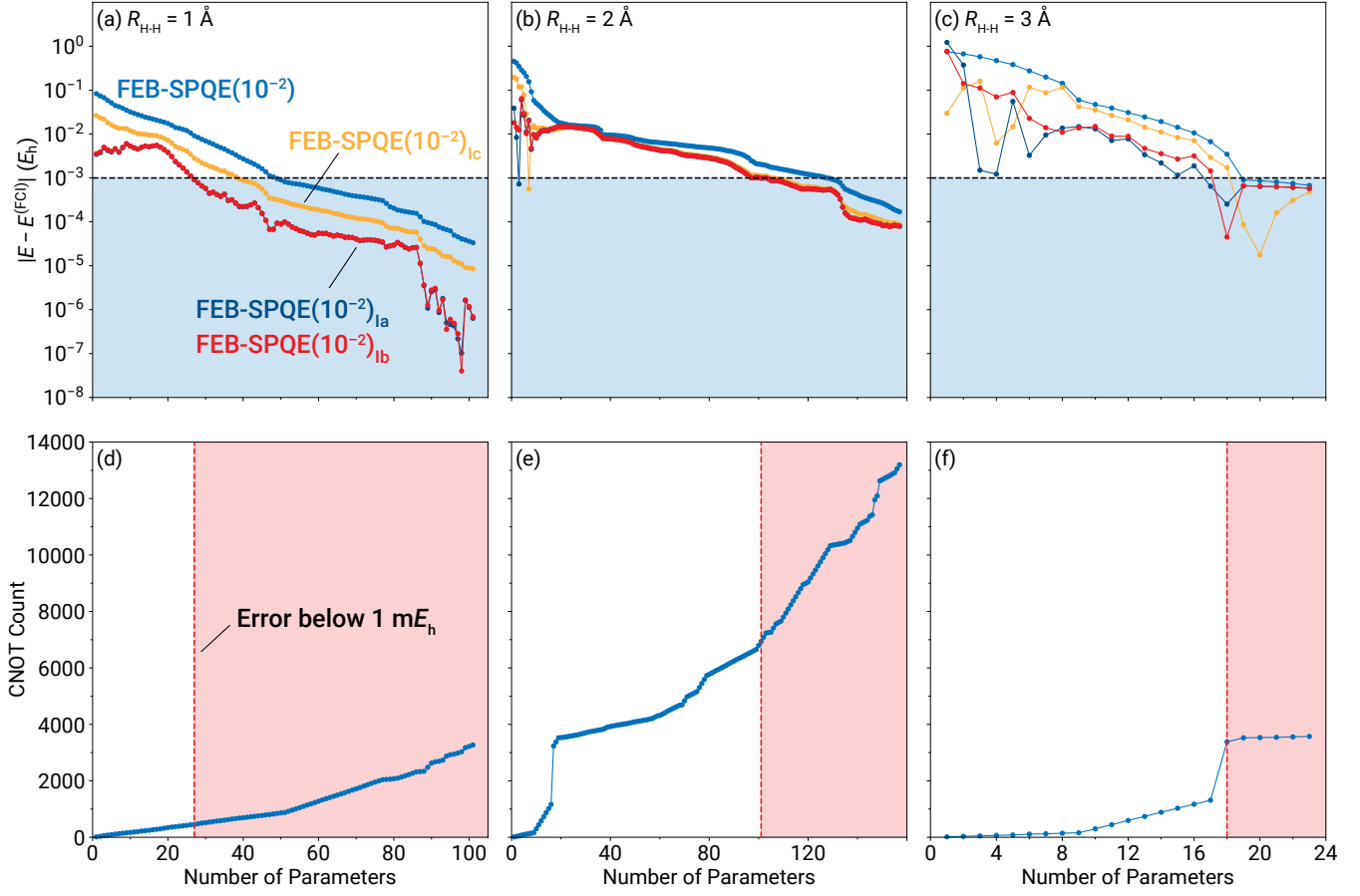


Figure 1: Errors relative to FCI [(a)–(c)] and CNOT gate counts [(d)–(f)] characterizing the FEB-SPQE simulations of the symmetric dissociation of the $H_6/STO-6G$ linear chain at three representative distances between neighboring H atoms, including $R_{H-H} = 1.0 \text{ \AA}$ [(a) and (d)], $R_{H-H} = 2.0 \text{ \AA}$ [(b) and (e)], and $R_{H-H} = 3.0 \text{ \AA}$ [(c) and (f)]. The blue-shaded area in the top-row panels indicates results within chemical accuracy ($1 mE_h$) from FCI. The red-shaded area in the bottom-row panels denotes the CNOT counts of the underlying FEB-SPQE quantum circuits for which the FEB-SPQE_{lb} energies are within chemical accuracy.

even further. However, since the contribution of the symmetry contaminants to the aFEB-SPQE wavefunction is negligible,⁵¹ we did not consider such a generalized correction.

Next, we examine the usefulness of the δ_{lb} non-iterative correction in the context of ADAPT-VQE (QEB-ADAPT-VQE_{lb}) and compare the results with those of aFEB-SPQE_{lb}. When examining the errors with respect to FCI, we observe that, in general, the QEB-ADAPT-VQE_{lb} approach offers a major improvement over the underlying QEB-ADAPT-VQE energetics (top panels to Figure 2). This enables QEB-ADAPT-VQE_{lb} to recover the FCI data within $1.0 mE_h$ faster than the underlying QEB-ADAPT-VQE approach, resulting in substantial savings in terms of CNOTs (see bottom panels to Figure 2). Exception to this is the QEB-ADAPT-VQE simulation for the strongly correlated regime of H_6 . In this case, QEB-ADAPT-VQE is characterized by a very slow convergence to FCI, most likely due to the presence of a local

energy minimum. For QEB-ADAPT-VQE_{lb}, this manifests itself as a plateau in the corresponding energies. The fact that after about 120 parameters the QEB-ADAPT-VQE and QEB-ADAPT-VQE_{lb} results practically coincide, i.e., the QEB-ADAPT-VQE moments are close to zero, further corroborates to the fact that the QEB-ADAPT-VQE wavefunction closely resembles that of an exact excited electronic state. Eventually both QEB-ADAPT-VQE and QEB-ADAPT-VQE_{lb} achieve chemical accuracy at the same time, requiring about 80% of the number of parameters of FCI.

Moving on to the comparison of the ADAPT-VQE and SPQE approaches, a quick inspection of the top panels to Figure 2 immediately reveals that aFEB-SPQE provides, in general, more accurate energetics than QEB-ADAPT-VQE for the same number of parameters. Similar behavior is observed when we examine their MMCC-corrected counterparts. The fact that aFEB-SPQE_{lb} is characterized by a faster convergence to FCI than

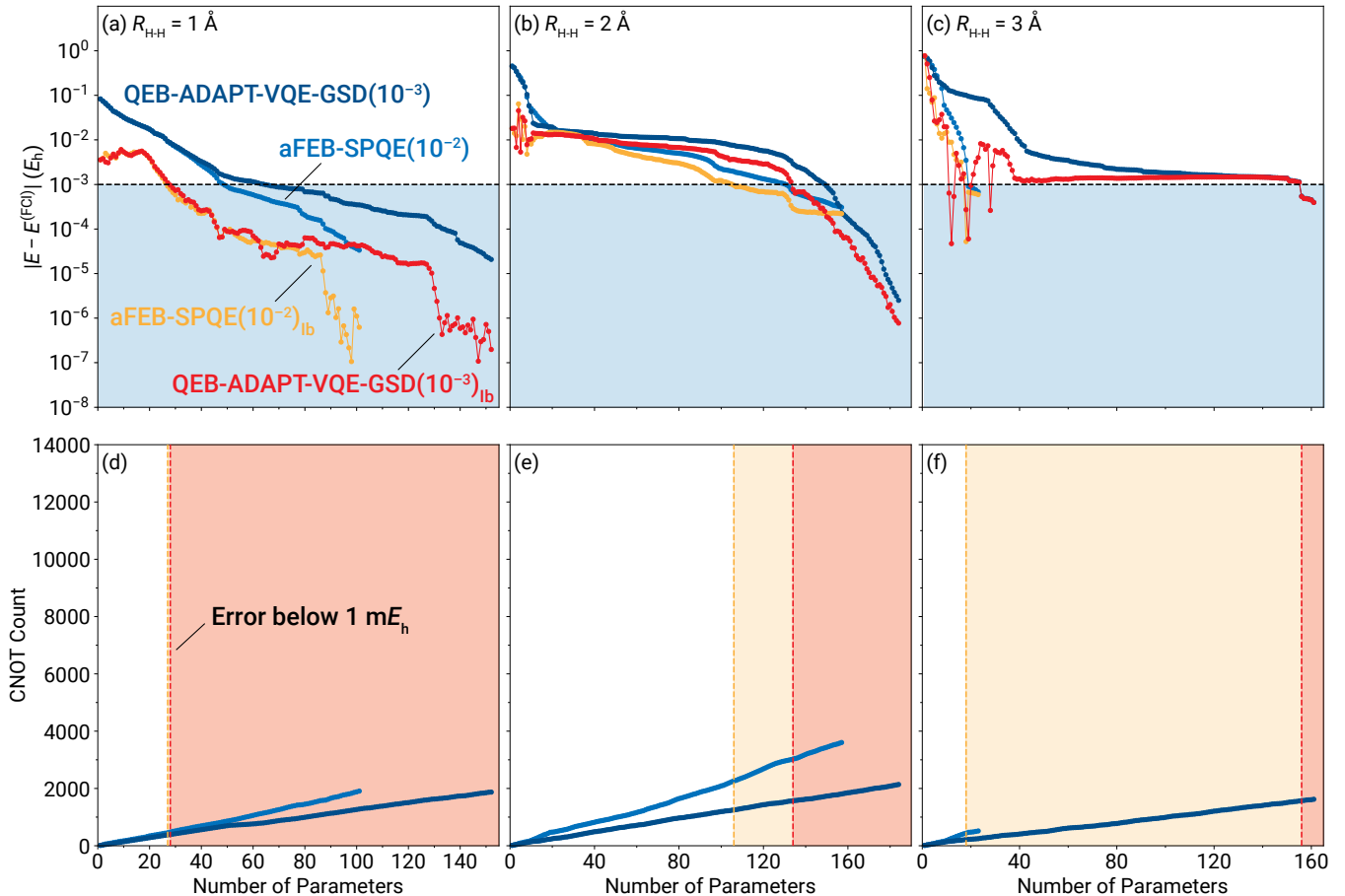


Figure 2: Errors relative to FCI [(a)–(c)] and CNOT gate counts [(d)–(f)] characterizing the aFEB-SPQE and QEB-ADAPT-VQE-GSD simulations of the symmetric dissociation of the H_6 /STO-6G linear chain at three representative distances between neighboring H atoms, including $R_{H-H} = 1.0 \text{ \AA}$ [(a) and (d)], $R_{H-H} = 2.0 \text{ \AA}$ [(b) and (e)], and $R_{H-H} = 3.0 \text{ \AA}$ [(c) and (f)]. The blue-shaded area in the top-row panels indicates results within chemical accuracy ($1 mE_h$) from FCI. The yellow- and red-shaded areas in the bottom-row panels denotes the CNOT counts of the underlying aFEB-SPQE and QEB-ADAPT-VQE-GSD quantum circuits, respectively, for which the aFEB-SPQE_{lb} and QEB-ADAPT-VQE-GSD_{lb} energetics are within chemical accuracy.

QEB-ADAPT-VQE_{lb} does not necessarily guarantee that it does so with fewer number of CNOTs. As demonstrated in the bottom panels to Figure 2, although both aFEB-SPQE and QEB-ADAPT-VQE generate quantum circuits with CNOT counts that scale, more or less, linearly with the number of parameters, the prefactor is smaller in the case of QEB-ADAPT-VQE. Indeed, for the three examined geometries of H_6 , characterized by the R_{H-H} values of 1.0 \AA , 2.0 \AA , and 3.0 \AA , QEB-ADAPT-VQE_{lb} attains chemical accuracy with the same, less, and more CNOTs, respectively, than when aFEB-SPQE_{lb} does.

Now we turn our attention to the δ_{II} MMCC-type correction, given by eq (16). To gauge the performance of this correction, we considered the UCCSD_{II} scheme in which we corrected the VQE UCCSD energies using the wavefunctions resulting from each macro-iteration defining the QEB-ADAPT-VQE simulations. The reason we opted

to use QEB-ADAPT-VQE as the external source of the wavefunction rather than aFEB-SPQE is that, for the same number of parameters, the former generates the most CNOT-efficient circuits. In Figure 3, we present the errors relative to FCI characterizing the UCCSD_{II} method and the underlying QEB-ADAPT-VQE approach. As depicted in Figure 3, with the exception of the very early stages of the QEB-ADAPT-VQE simulations, in which UCCSD is more accurate, UCCSD_{II} consistently outperforms both UCCSD and QEB-ADAPT-VQE. As far as the number of CNOTs needed to achieve chemical accuracy is concerned, which of the UCCSD and QEB-ADAPT-VQE requires the deepest circuit depends on the strength of the correlation effects. Based on our numerical results for H_6 , in the weakly and strongly correlated regions, where UCCSD_{II} recovers the FCI energies within $1.0 mE_h$ rather quickly, UCCSD is the bottleneck in terms of CNOT count. The situation

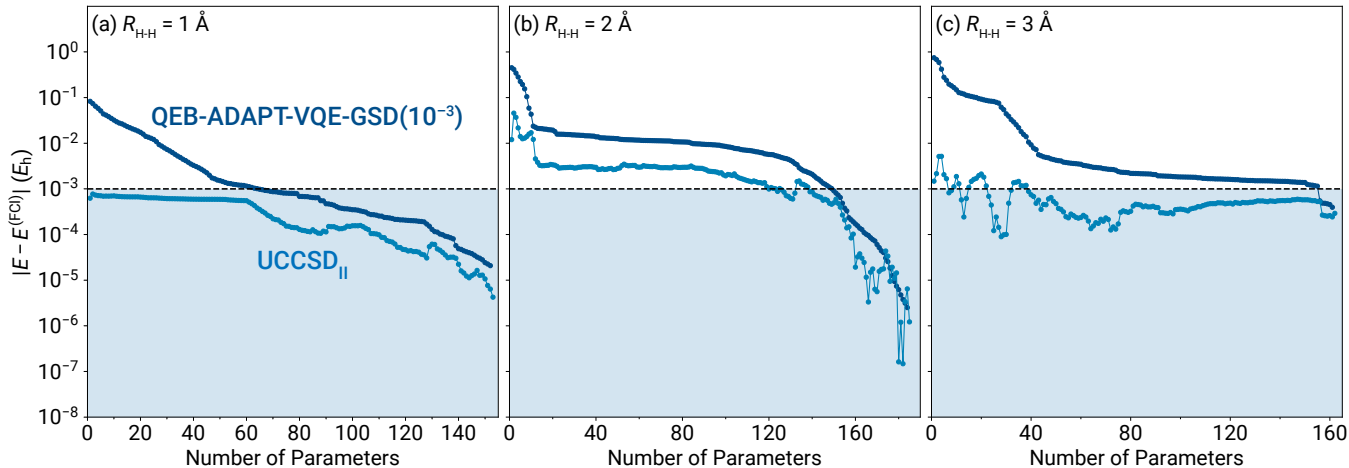


Figure 3: Errors relative to FCI characterizing the moment-corrected UCCSD_{II} scheme and the underlying QEB-ADAPT-VQE-GSD simulations of the symmetric dissociation of the H₆/STO-6G linear chain at three representative distances between neighboring H atoms, including (a) $R_{\text{H-H}} = 1.0 \text{ \AA}$, (b) $R_{\text{H-H}} = 2.0 \text{ \AA}$, and (c) $R_{\text{H-H}} = 3.0 \text{ \AA}$. The blue-shaded area indicates results within chemical accuracy ($1 \text{ m}E_h$) from FCI.

changes when we examine the recoupling region, in which case QEB-ADAPT-VQE defines the overall CNOT cost. In comparing the UCCSD_{II} and QEB-ADAPT-VQE_{IB} approaches among themselves, we observe that UCCSD_{II} is characterized by a more rapid convergence to FCI. This can be mostly attributed to the fact that UCCSD offers a good starting point for the MMCC-type correction, especially so during the early stages of the simulation.

In this work, we explored the usefulness of moment expansions, used in the past to define the renormalized and completely renormalized CC approaches, to construct non-iterative corrections to the energies obtained with hybrid quantum-classical algorithms employing a UCC ansatz. In an attempt to minimize the circuit depth, we combined the non-iterative energy corrections with iteratively constructed ansätze and CNOT-efficient implementations of quantum circuits. Our preliminary numerical results for three representative geometries along the potential energy curve characterizing the symmetric dissociation of the H₆ linear chain are very encouraging. All of the examined corrections accelerated the convergence to FCI of the underlying quantum algorithms, resulting in substantial savings in terms of CNOT gates. The performance of the aFEB-SPQE_{IB}, QEB-ADAPT-VQE_{IB}, and UCCSD_{II} is particularly promising. We point out that the corrections studied in this work are applicable even when the trial state is not of the UCC form, opening the possibility to improve hardware efficient ansätze and other trial states that are not expressible via the UCC form. In the future, we will explore the flexibility of the

δ_{II} correction, combining different types of trial and external wavefunctions. Finally, inspired by the success of MMCC-type corrections for excited electronic states,^{61,63,66,113–118} we plan to investigate this aspect as well.

Acknowledgement This work is supported by the U.S. Department of Energy under Award No. DE-SC0019374.

Supporting Information Available

Proof of the size consistency of the non-iterative corrections and additional numerical results. Numerical data generated in this study.

References

- (1) Lanyon, B. P.; Whitfield, J. D.; Gillet, G. G.; Goggin, M. E.; Almeida, M. P.; Kassal, I.; Biamonte, J. D.; Mohseni, M.; Powell, B. J.; Barbieri, M. et al. Towards Quantum Chemistry on a Quantum Computer. *Nat. Chem.* **2010**, *2*, 106–111, DOI: 10.1038/NCHEM.483.
- (2) Bharti, K.; Cerveta-Liarta, A.; Kyaw, T. H.; Haug, T.; Alperin-Lea, S.; Anand, A.; Degroote, M.; Heimonen, H.; Kottmann, J. S.; Menke, T. et al. Noisy Intermediate-Scale Quantum Algorithms. *Rev. Mod. Phys.* **2022**, *94*, 015004, DOI: 10.1103/RevModPhys.94.015004.

- (3) Endo, S.; Cai, Z.; Benjamin, S. C.; Yuan, X. Hybrid Quantum-Classical Algorithms and Quantum Error Mitigation. *J. Phys. Soc. Jpn.* **2021**, *90*, 032001, DOI: 10.7566/JPSJ.90.032001.
- (4) Callison, A.; Chancellor, N. Hybrid Quantum Classical Algorithms in the Noisy Intermediate-Scale Quantum Era and Beyond. *Phys. Rev. A* **2022**, *106*, 010101, DOI: 10.1103/PhysRevA.106.010101.
- (5) Peruzzo, A.; McClean, J.; Shadbolt, P.; Yung, M.-H.; Zhou, X.-Q.; Love, P. J.; Aspuru-Guzik, A.; O'Brien, J. L. A Variational Eigenvalue Solver on a Photonic Quantum Processor. *Nat. Commun.* **2014**, *5*, 4213, DOI: 10.1038/ncomms5213.
- (6) McClean, J. R.; Romero, J.; Babbush, R.; Aspuru-Guzik, A. The Theory of Variational Quantum-Classical Algorithms. *New J. Phys.* **2016**, *18*, 023023, DOI: 10.1088/1367-2630/18/2/023023.
- (7) Cerezo, M.; Arrasmith, A.; Babbush, R.; Benjamin, S. C.; Endo, S.; Fujii, K.; McClean, J. R.; Mitarai, K.; Yuan, X.; Cincio, L. et al. Variational Quantum Algorithms. *Nat. Rev. Phys.* **2021**, *3*, 625–644, DOI: 10.1038/s42254-021-00348-9.
- (8) Tilly, J.; Chen, H.; Cao, S.; Picozzi, D.; Setia, K.; Li, Y.; Grant, E.; Wossnig, L.; Rungger, I.; Booth, G. H. et al. The Variational Quantum Eigensolver: A Review of Methods and Best Practices. *Phys. Rep.* **2022**, *986*, 1–128, DOI: 10.1016/j.physrep.2022.08.003.
- (9) Fedorov, D. A.; Peng, B.; Govind, N.; Alexeev, Y. VQE Method: A Short Survey and Recent Developments. *Mater. Theory* **2022**, *6*, 2, DOI: 10.1186/s41313-021-00032-6.
- (10) Smart, S. E.; Mazziotti, D. A. Quantum Solver of Contracted Eigenvalue Equations for Scalable Molecular Simulations on Quantum Computing Devices. *Phys. Rev. Lett.* **2021**, *126*, 070504, DOI: 10.1103/PhysRevLett.126.070504.
- (11) Stair, N. H.; Evangelista, F. A. Simulating Many-Body Systems with a Projective Quantum Eigensolver. *PRX Quantum* **2021**, *2*, 030301, DOI: 10.1103/PRXQuantum.2.030301.
- (12) Motta, M.; Sun, C.; Tan, A. T. K.; O'Rourke, M. J.; Ye, E.; Minnich, A. J.; ao, F. G. S. L. B.; Chan, G. K.-L. Determining Eigenstates and Thermal States on a Quantum Computer Using Quantum Imaginary Time Evolution. *Nat. Phys.* **2020**, *16*, 205–210, DOI: 10.1038/s41567-019-0704-4.
- (13) Sun, S.-N.; Motta, M.; Tazhigulov, R. N.; Tan, A. T. K.; Chan, G. K.-L.; Minnich, A. J. Quantum Computation of Finite-Temperature Static and Dynamical Properties of Spin Systems Using Quantum Imaginary Time Evolution. *PRX Quantum* **2021**, *2*, 010317, DOI: 10.1103/PRXQuantum.2.010317.
- (14) McClean, J. R.; Kimchi-Schwartz, M. E.; Carter, J.; de Jong, W. A. Hybrid Quantum-Classical Hierarchy for Mitigation of Decoherence and Determination of Excited States. *Phys. Rev. A* **2017**, *95*, 042308, DOI: 10.1103/PhysRevA.95.042308.
- (15) Parrish, R. M.; McMahan, P. L. Quantum Filter Diagonalization: Quantum Eigendecomposition without Full Quantum Phase Estimation. 2019, arXiv:1909.08925v1. arXiv.org e-Print archive. <https://arxiv.org/abs/1909.08925v1>.
- (16) Stair, N. H.; Huang, R.; Evangelista, F. A. A Multireference Quantum Krylov Algorithm for Strongly Correlated Electrons. *J. Chem. Theory Comput.* **2020**, *16*, 2236–2245, DOI: 10.1021/acs.jctc.9b01125.
- (17) Huggins, W. J.; Lee, J.; Baek, U.; O'Gorman, B.; Whaley, K. B. A Non-Orthogonal Variational Quantum Eigensolver. *New J. Phys.* **2020**, *22*, 073009, DOI: 10.1088/1367-2630/ab867b.
- (18) Kitaev, A. Y. Quantum Measurements and the Abelian Stabilizer Problem. 1995, arXiv:quant-ph/9511026. arXiv.org e-Print archive. <https://arxiv.org/abs/quant-ph/9511026>.

- (19) Abrams, D. S.; Lloyd, S. Simulation of Many-Body Fermi Systems on a Universal Quantum Computer. *Phys. Rev. Lett.* **1997**, *79*, 2586–2589, DOI: 10.1103/PhysRevLett.79.2586.
- (20) Abrams, D. S.; Lloyd, S. Quantum Algorithm Providing Exponential Speed Increase for Finding Eigenvalues and Eigenvectors. *Phys. Rev. Lett.* **1999**, *83*, 5162–5165, DOI: 10.1103/PhysRevLett.83.5162.
- (21) Grimsley, H. R.; Economou, S. E.; Barnes, E.; Mayhall, N. J. An Adaptive Variational Algorithm for Exact Molecular Simulations on a Quantum Computer. *Nat Commun.* **2019**, *10*, 3007, DOI: 10.1038/s41467-019-10988-2.
- (22) Tang, H. L.; Shkolnikov, V. O.; Barron, G. S.; Grimsley, H. R.; Mayhall, N. J.; Barnes, E.; Economou, S. E. Qubit-ADAPT-VQE: An Adaptive Algorithm for Constructing Hardware-Efficient Ansätze on a Quantum Processor. *PRX Quantum* **2021**, *2*, 020310, DOI: 10.1103/PRXQuantum.2.020310.
- (23) Yordanov, Y. S.; Armaos, V.; Barnes, C. H. W.; Arvidsson-Shukur, D. R. M. Qubit-Excitation-Based Adaptive Variational Quantum Eigensolver. *Commun. Phys.* **2021**, *4*, 228, DOI: 10.1038/s42005-021-00730-0.
- (24) Ryabinkin, I. G.; Lang, R. A.; Genin, S. N.; Izmaylov, A. F. Iterative Qubit Coupled Cluster Approach with Efficient Screening of Generators. *J. Chem. Theory Comput.* **2020**, *16*, 1055–1063, DOI: 10.1021/acs.jctc.9b01084.
- (25) Mazziotti, D. A.; Smart, S. E.; Mazziotti, A. R. Quantum Simulation of Molecules without Fermionic Encoding of the Wave Function. *New J. Phys.* **2021**, *23*, 113037, DOI: 10.1088/1367-2630/ac3573.
- (26) Smart, S. E.; Mazziotti, D. A. Many-Fermion Simulation from the Contracted Quantum Eigensolver without Fermionic Encoding of the Wave Function. *Phys. Rev. A* **2022**, *105*, 062424, DOI: 10.1103/PhysRevA.105.062424.
- (27) Fedorov, D. A.; Alexeev, Y.; Gray, S. K.; Otten, M. J. Unitary Selective Coupled-Cluster Method. *Quantum* **2022**, *6*, 703, DOI: 10.22331/q-2022-05-02-703.
- (28) Kutzelnigg, W. In *Methods of Electronic Structure Theory*; Schaefer, H. F., III, Ed.; Springer: Boston, 1977; pp 129–188, DOI: 10.1007/978-1-4757-0887-5_5.
- (29) Kutzelnigg, W. Quantum Chemistry in Fock Space. I. The Universal Wave and Energy Operators. *J. Chem. Phys.* **1982**, *77*, 3081–3097, DOI: 10.1063/1.444231.
- (30) Kutzelnigg, W.; Koch, S. Quantum Chemistry in Fock Space. II. Effective Hamiltonians in Fock Space. *J. Chem. Phys.* **1983**, *79*, 4315–4335, DOI: 10.1063/1.446313.
- (31) Kutzelnigg, W. Quantum Chemistry in Fock Space. III. Particle-Hole Formalism. *J. Chem. Phys.* **1984**, *80*, 822–830, DOI: 10.1063/1.446736.
- (32) Bartlett, R. J.; Kucharski, S. A.; Noga, J. Alternative Coupled-Cluster Ansätze II. The Unitary Coupled-Cluster Method. *Chem. Phys. Lett.* **1989**, *155*, 133–140, DOI: 10.1016/S0009-2614(89)87372-5.
- (33) Szalay, P. G.; Nooijen, M.; Bartlett, R. J. Alternative Ansätze in Single Reference Coupled-Cluster Theory. III. A Critical Analysis of Different Methods. *J. Chem. Phys.* **1995**, *103*, 281–298, DOI: 10.1063/1.469641.
- (34) Taube, A. G.; Bartlett, R. J. New Perspectives on Unitary Coupled-Cluster Theory. *Int. J. Quantum Chem.* **2006**, *106*, 3393–3401, DOI: 10.1002/qua.21198.
- (35) Cooper, B.; Knowles, P. J. Benchmark Studies of Variational, Unitary and Extended Coupled Cluster Methods. *J. Chem. Phys.* **2010**, *133*, 234102, DOI: 10.1063/1.3520564.
- (36) Evangelista, F. A. Alternative Single-Reference Coupled Cluster Approaches for Multireference Problems: The Simpler, the Better. *J. Chem. Phys.* **2011**, *134*, 224102, DOI: 10.1063/1.3598471.

- (37) Harsha, G.; Shiozaki, T.; Scuseria, G. E. On the Difference Between Variational and Unitary Coupled Cluster Theories. *J. Chem. Phys.* **2018**, *148*, 044107, DOI: 10.1063/1.5011033.
- (38) Filip, M.-A.; Thom, A. J. W. A Stochastic Approach to Unitary Coupled Cluster. *J. Chem. Phys.* **2020**, *153*, 214106, DOI: 10.1063/5.0026141.
- (39) Freericks, J. K. Operator Relationship between Conventional Coupled Cluster and Unitary Coupled Cluster. *Symmetry* **2022**, *14*, 494, DOI: 10.3390/sym14030494.
- (40) Anand, A.; Schleich, P.; Alperin-Lea, S.; Jensen, P. W. K.; Sim, S.; Diaz-Tinoco, M.; Kottmann, J. S.; Degroote, M.; Izmaylov, A. F.; Aspuru-Guzik, A. A Quantum Computing View on Unitary Coupled Cluster Theory. *Chem. Soc. Rev.* **2022**, *51*, 1659–1684, DOI: 10.1039/d1cs00932j.
- (41) Coester, F. Bound States of a Many-Particle System. *Nucl. Phys.* **1958**, *7*, 421–424, DOI: 10.1016/0029-5582(58)90280-3.
- (42) Coester, F.; Kümmel, H. Short-Range Correlations in Nuclear Wave Functions. *Nucl. Phys.* **1960**, *17*, 477–485, DOI: 10.1016/0029-5582(60)90140-1.
- (43) Čížek, J. On the Correlation Problem in Atomic and Molecular Systems. Calculation of Wavefunction Components in Ursell-Type Expansion Using Quantum-Field Theoretical Methods. *J. Chem. Phys.* **1966**, *45*, 4256–4266, DOI: 10.1063/1.1727484.
- (44) Čížek, J. On the Use of the Cluster Expansion and the Technique of Diagrams in Calculations of Correlation Effects in Atoms and Molecules. *Adv. Chem. Phys.* **1969**, *14*, 35–89, DOI: 10.1002/9780470143599.ch2.
- (45) Čížek, J.; Paldus, J. Correlation Problems in Atomic and Molecular Systems III. Rederivation of the Coupled-Pair Many-Electron Theory Using the Traditional Quantum Chemical Methods. *Int. J. Quantum Chem.* **1971**, *5*, 359–379, DOI: 10.1002/qua.560050402.
- (46) Paldus, J.; Čížek, J.; Shavitt, I. Correlation Problems in Atomic and Molecular Systems. IV. Extended Coupled-Pair Many-Electron Theory and Its Application to the BH₃ Molecule. *Phys. Rev. A* **1972**, *5*, 50–67, DOI: 10.1103/PhysRevA.5.50.
- (47) Ryabinkin, I. G.; Yen, T.-C.; Genin, S. N.; Izmaylov, A. F. Qubit Coupled Cluster Method: A Systematic Approach to Quantum Chemistry on a Quantum Computer. *J. Chem. Theory Comput.* **2018**, *14*, 6317–6326, DOI: 10.1021/acs.jctc.8b00932.
- (48) Yordanov, Y. S.; Arvidsson-Shukur, D. R. M.; Barnes, C. H. W. Efficient Quantum Circuits for Quantum Computational Chemistry. *Phys. Rev. A* **2020**, *102*, 062612, DOI: 10.1103/PhysRevA.102.062612.
- (49) Xia, R.; Kais, S. Qubit Coupled Cluster Singles and Doubles Variational Quantum Eigensolver Ansatz for Electronic Structure Calculations. *Quantum Sci. Technol.* **2021**, *6*, 015001, DOI: 10.1088/2058-9565/abb74.
- (50) Magoulas, I.; Evangelista, F. A. CNOT-Efficient Quantum Circuits for Arbitrary Rank Many-Body Fermionic and Qubit Excitations. *J. Chem. Theory Comput.* **2023**, *19*, 822–836, DOI: 10.1021/acs.jctc.2c01016.
- (51) Magoulas, I.; Evangelista, F. A. Linear-Scaling Quantum Circuits for Computational Chemistry. 2023, arXiv:2304.12870. arXiv.org e-Print archive. <https://arxiv.org/abs/2304.12870>.
- (52) Ryabinkin, I. G.; Izmaylov, A. F.; Genin, S. N. *A Posteriori* Corrections to the Iterative Qubit Coupled Cluster Method to Minimize the Use of Quantum Resources in Large-Scale Calculations. *Quantum Sci. Technol.* **2021**, *6*, 024012, DOI: 10.1088/2058-9565/abda8e.
- (53) Piecuch, P.; Kowalski, K. In *Computational Chemistry: Reviews of Current Trends*; Leszczyński, J., Ed.; World Scientific: Singapore, 2000; Vol. 5; pp 1–104, DOI: 10.1142/9789812792501_0001.

- (54) Kowalski, K.; Piecuch, P. The Method of Moments of Coupled-Cluster Equations and the Renormalized CCSD[T], CCSD(T), CCSD(TQ), and CCSDT(Q) Approaches. *J. Chem. Phys.* **2000**, *113*, 18–35, DOI: 10.1063/1.481769.
- (55) Kowalski, K.; Piecuch, P. Renormalized CCSD(T) and CCSD(TQ) Approaches: Dissociation of the N₂ Triple Bond. *J. Chem. Phys.* **2000**, *113*, 5644–5652, DOI: 10.1063/1.1290609.
- (56) Piecuch, P.; Kucharski, S. A.; Kowalski, K. Can Ordinary Single-Reference Coupled-Cluster Methods Describe the Potential Energy Curve of N₂? The Renormalized CCSDT(Q) Study. *Chem. Phys. Lett.* **2001**, *344*, 176–184, DOI: 10.1016/S0009-2614(01)00759-X.
- (57) Fan, P.-D.; Kowalski, K.; Piecuch, P. Non-Iterative Corrections to Extended Coupled-Cluster Energies Employing the Generalized Method of Moments of Coupled-Cluster Equations. *Mol. Phys.* **2005**, *103*, 2191–2213, DOI: 10.1080/00268970500131595.
- (58) Lodriguito, M. D.; Kowalski, K.; Włoch, M.; Piecuch, P. Non-Iterative Coupled-Cluster Methods Employing Multi-Reference Perturbation Theory Wave Functions. *J. Mol. Struct.: THEOCHEM* **2006**, *771*, 89–104, DOI: 10.1016/j.theochem.2006.03.014.
- (59) Piecuch, P.; Włoch, M. Renormalized Coupled-Cluster Methods Exploiting Left Eigenstates of the Similarity-Transformed Hamiltonian. *J. Chem. Phys.* **2005**, *123*, 224105, DOI: 10.1063/1.2137318.
- (60) Piecuch, P.; Włoch, M.; Gour, J. R.; Kinal, A. Single-Reference, Size-Extensive, Non-Iterative Coupled-Cluster Approaches to Bond Breaking and Biradicals. *Chem. Phys. Lett.* **2006**, *418*, 467–474, DOI: 10.1016/j.cpllett.2005.10.116.
- (61) Włoch, M.; Lodriguito, M. D.; Piecuch, P.; Gour, J. R. Two New Classes of Non-Iterative Coupled-Cluster Methods Derived from the Method of Moments of Coupled-Cluster Equations. *Mol. Phys.* **2006**, *104*, 2149–2172, DOI: 10.1080/00268970600659586, *ibid.* **124**, 2291 (2006) [Erratum].
- (62) Włoch, M.; Gour, J. R.; Piecuch, P. Extension of the Renormalized Coupled-Cluster Methods Exploiting Left Eigenstates of the Similarity-Transformed Hamiltonian to Open-Shell Systems: A Benchmark Study. *J. Phys. Chem. A* **2007**, *111*, 11359–11382, DOI: 10.1021/jp0725351.
- (63) Piecuch, P.; Gour, J. R.; Włoch, M. Left-Eigenstate Completely Renormalized Equation-of-Motion Coupled-Cluster Methods: Review of Key Concepts, Extension to Excited States of Open-Shell Systems, and Comparison with Electron-Attached and Ionized Approaches. *Int. J. Quantum Chem.* **2009**, *109*, 3268–3304, DOI: 10.1002/qua.22367.
- (64) Piecuch, P.; Kowalski, K.; Pimienta, I. S. O.; McGuire, M. J. Recent Advances in Electronic Structure Theory: Method of Moments of Coupled-Cluster Equations and Renormalized Coupled-Cluster Approaches. *Int. Rev. Phys. Chem.* **2002**, *21*, 527–655, DOI: 10.1080/0144235021000053811.
- (65) Piecuch, P.; Kowalski, K.; Pimienta, I. S. O.; Fan, P.-D.; Lodriguito, M.; McGuire, M. J.; Kucharski, S. A.; Kuś, T.; Musiał, M. Method of Moments of Coupled-Cluster Equations: A New Formalism for Designing Accurate Electronic Structure Methods for Ground and Excited States. *Theor. Chem. Acc.* **2004**, *112*, 349–393, DOI: 10.1007/s00214-004-0567-2.
- (66) Shen, J.; Piecuch, P. Biorthogonal Moment Expansions in Coupled-Cluster Theory: Review of Key Concepts and Merging the Renormalized and Active-Space Coupled-Cluster Methods. *Chem. Phys.* **2012**, *401*, 180–202, DOI: 10.1016/j.chemphys.2011.11.033.
- (67) Urban, M.; Noga, J.; Cole, S. J.; Bartlett, R. J. Towards a Full CCSDT Model for Electron Correlation. *J. Chem. Phys.* **1985**, *83*, 4041–4046, DOI: 10.1063/1.449067, *ibid.* **85**, 5383 (1986) [Erratum].

- (68) Raghavachari, K. An Augmented Coupled Cluster Method and Its Application to the First-Row Homonuclear Diatomics. *J. Chem. Phys.* **1985**, *82*, 4607–4610, DOI: 10.1063/1.448718.
- (69) Raghavachari, K.; Trucks, G. W.; Pople, J. A.; Head-Gordon, M. A Fifth-Order Perturbation Comparison of Electron Correlation Theories. *Chem. Phys. Lett.* **1989**, *157*, 479–483, DOI: 10.1016/S0009-2614(89)87395-6.
- (70) Kucharski, S. A.; Bartlett, R. J. Coupled-Cluster Methods that Include Connected Quadruple Excitations, T_4 : CCSDTQ-1 and Q(CCSDT). *Chem. Phys. Lett.* **1989**, *158*, 550–555, DOI: 10.1016/0009-2614(89)87388-9.
- (71) Bartlett, R. J.; Watts, J. D.; Kucharski, S. A.; Noga, J. Non-Iterative Fifth-Order Triple and Quadruple Excitation Energy Corrections in Correlated Methods. *Chem. Phys. Lett.* **1990**, *165*, 513–522, DOI: 10.1016/0009-2614(90)87031-L.
- (72) Kucharski, S. A.; Bartlett, R. J. Coupled-Cluster Methods Correct through Sixth Order. *Chem. Phys. Lett.* **1993**, *206*, 574–583, DOI: 10.1016/0009-2614(93)80186-S.
- (73) Kucharski, S. A.; Bartlett, R. J. Noniterative Energy Corrections Through Fifth-Order to the Coupled Cluster Singles and Doubles Method. *J. Chem. Phys.* **1998**, *108*, 5243–5254, DOI: 10.1063/1.475961.
- (74) Kucharski, S. A.; Bartlett, R. J. Sixth-Order Energy Corrections with Converged Coupled Cluster Singles and Doubles Amplitudes. *J. Chem. Phys.* **1998**, *108*, 5255–5264, DOI: 10.1063/1.475962.
- (75) Kucharski, S. A.; Bartlett, R. J. An Efficient Way to Include Connected Quadruple Contributions into the Coupled Cluster Method. *J. Chem. Phys.* **1998**, *108*, 9221–9226, DOI: 10.1063/1.476376.
- (76) Musial, M.; Kucharski, S. A.; Bartlett, R. J. T_5 Operator in Coupled Cluster Calculations. *Chem. Phys. Lett.* **2000**, *320*, 542–548, DOI: 10.1016/S0009-2614(00)00290-6.
- (77) Peng, B.; Kowalski, K. Mapping Renormalized Coupled Cluster Methods to Quantum Computers through a Compact Unitary Representation of Nonunitary Operators. *Phys. Rev. Research* **2022**, *4*, 043172, DOI: 10.1103/PhysRevResearch.4.043172.
- (78) Schuld, M.; Bergholm, V.; Gogolin, C.; Izaac, J.; Killoran, N. Evaluating Analytic Gradients on Quantum Hardware. *Phys. Rev. A* **2019**, *99*, 032331, DOI: 10.1103/PhysRevA.99.032331.
- (79) Kottmann, J. S.; Anand, A.; Aspuru-Guzik, A. A Feasible Approach for Automatically Differentiable Unitary Coupled-Cluster on Quantum Computers. *Chem. Sci.* **2021**, *12*, 3497–3508, DOI: 10.1039/d0sc06627c.
- (80) Jankowski, K.; Paldus, J.; Piecuch, P. Method of Moments Approach and Coupled Cluster Theory. *Theor. Chim. Acta* **1991**, *80*, 223–243, DOI: 10.1007/BF01117411.
- (81) Shen, J.; Piecuch, P. Combining Active-Space Coupled-Cluster Methods with Moment Energy Corrections via the CC($P;Q$) Methodology, with Benchmark Calculations for Biradical Transition States. *J. Chem. Phys.* **2012**, *136*, 144104, DOI: 10.1063/1.3700802.
- (82) Shen, J.; Piecuch, P. Merging Active-Space and Renormalized Coupled-Cluster Methods via the CC($P;Q$) Formalism, with Benchmark Calculations for Singlet–Triplet Gaps in Biradical Systems. *J. Chem. Theory Comput.* **2012**, *8*, 4968–4988, DOI: 10.1021/ct300762m.
- (83) Stanton, J. F. Why CCSD(T) Works: A Different Perspective. *Chem. Phys. Lett.* **1997**, *281*, 130–134, DOI: 10.1016/S0009-2614(97)01144-5.
- (84) Huron, B.; Malrieu, J.-P.; Rancurel, P. Iterative Perturbation Calculations of Ground and Excited State Energies from Multiconfigurational Zeroth-Order Wavefunctions. *J. Chem. Phys.* **1973**, *58*, 5745–5759, DOI: 10.1063/1.1679199.
- (85) Garniron, Y.; Scemama, A.; Loos, P.-F.; Caffarel, M. Hybrid stochastic-deterministic

- calculation of the second-order perturbative contribution of multireference perturbation theory. *J. Chem. Phys.* **2017**, *147*, 034101, DOI: 10.1063/1.4992127.
- (86) Garniron, Y.; Applencourt, T.; Gasperich, K.; Benali, A.; Ferte, A.; Paquier, J.; Pradines, B.; Assaraf, R.; Reinhardt, P.; Toulouse, J. et al. Quantum Package 2.0: An Open-Source Determinant-Driven Suite of Programs. *J. Chem. Theory Comput.* **2019**, *15*, 3591–3609, DOI: 10.1021/acs.jctc.9b00176.
- (87) Schriber, J. B.; Evangelista, F. A. Communication: An Adaptive Configuration Interaction Approach for Strongly Correlated Electrons with Tunable Accuracy. *J. Chem. Phys.* **2016**, *144*, 161106, DOI: 10.1063/1.4948308.
- (88) Schriber, J. B.; Evangelista, F. A. Adaptive Configuration Interaction for Computing Challenging Electronic Excited States with Tunable Accuracy. *J. Chem. Theory Comput.* **2017**, *13*, 5354–5366, DOI: 10.1021/acs.jctc.7b00725.
- (89) Tubman, N. M.; Lee, J.; Takeshita, T. Y.; Head-Gordon, M.; Whaley, K. B. A Deterministic Alternative to the Full Configuration Interaction Quantum Monte Carlo Method. *J. Chem. Phys.* **2016**, *145*, 044112, DOI: 10.1063/1.4955109.
- (90) Paldus, J.; Čížek, J.; Takahashi, M. Approximate Account of the Connected Quadruply Excited Clusters in the Coupled-Pair Many-Electron Theory. *Phys. Rev. A* **1984**, *30*, 2193–2209, DOI: 10.1103/PhysRevA.30.2193.
- (91) Piecuch, P.; Paldus, J. Coupled Cluster Approaches with an Approximate Account of Triexcitations and the Optimized Inner Projection Technique. *Theor. Chim. Acta* **1990**, *78*, 65–128, DOI: 10.1007/BF01119191.
- (92) Piecuch, P.; Toboła, R.; Paldus, J. Approximate Account of Connected Quadruply Excited Clusters in Single-Reference Coupled-Cluster Theory via Cluster Analysis of the Projected Unrestricted Hartree-Fock Wave Function. *Phys. Rev. A* **1996**, *54*, 1210–1241, DOI: 10.1103/PhysRevA.54.1210.
- (93) Paldus, J.; Planelles, J. Valence Bond Corrected Single Reference Coupled Cluster Approach. *Theor. Chim. Acta* **1994**, *89*, 13–31, DOI: 10.1007/BF01123868.
- (94) Stolarczyk, L. Z. Complete Active Space Coupled-Cluster Method. Extension of Single-Reference Coupled-Cluster Method using the CASSCF Wavefunction. *Chem. Phys. Lett.* **1994**, *217*, 1–6, DOI: 10.1016/0009-2614(93)E1333-C.
- (95) Peris, G.; Planelles, J.; Paldus, J. Single-Reference CCSD Approach Employing Three- and Four-Body CAS SCF Corrections: A Preliminary Study of a Simple Model. *Int. J. Quantum Chem.* **1997**, *62*, 137–151, DOI: 10.1002/(SICI)1097-461X(1997)62:2<137::AID-QUA2>3.0.CO;2-X.
- (96) Peris, G.; Planelles, J.; Malrieu, J.-P.; Paldus, J. Perturbatively Selected CI as an Optimal Source for Externally Corrected CCSD. *J. Chem. Phys.* **1999**, *110*, 11708–11716, DOI: 10.1063/1.479116.
- (97) Li, X.; Paldus, J. Reduced Multireference CCSD Method: An Effective Approach to Quasidegenerate States. *J. Chem. Phys.* **1997**, *107*, 6257–6269, DOI: 10.1063/1.474289.
- (98) Li, X.; Paldus, J. Reduced Multireference Coupled Cluster Method with Singles and Doubles: Perturbative Corrections for Triples. *J. Chem. Phys.* **2006**, *124*, 174101, DOI: 10.1063/1.2194543.
- (99) Paldus, J. Externally and Internally Corrected Coupled Cluster Approaches: An Overview. *J. Math. Chem.* **2017**, *55*, 477–502, DOI: 10.1007/s10910-016-0688-6.
- (100) Deustua, J. E.; Magoulas, I.; Shen, J.; Piecuch, P. Communication: Approaching Exact Quantum Chemistry by Cluster Analysis of Full Configuration Interaction Quantum Monte Carlo Wave Functions. *J. Chem. Phys.* **2018**, *149*, 151101, DOI: 10.1063/1.5055769.
- (101) Aroeira, G. J. R.; Davis, M. M.; Turney, J. M.; Schaefer, H. F., III Coupled

- Cluster Externally Corrected by Adaptive Configuration Interaction. *J. Chem. Theory Comput.* **2021**, *17*, 182–190, DOI: 10.1021/acs.jctc.0c00888.
- (102) Magoulas, I.; Gururangan, K.; Piecuch, P.; Deustua, J. E.; Shen, J. Is Externally Corrected Coupled Cluster Always Better Than the Underlying Truncated Configuration Interaction? *J. Chem. Theory Comput.* **2021**, *17*, 4006–4027, DOI: 10.1021/acs.jctc.1c00181.
- (103) Hehre, W. J.; Stewart, R. F.; Pople, J. A. Self-Consistent Molecular-Orbital Methods. I. Use of Gaussian Expansions of Slater-Type Atomic Orbitals. *J. Chem. Phys.* **1969**, *51*, 2657–2664, DOI: 10.1063/1.1672392.
- (104) Deustua, J. E.; Shen, J.; Piecuch, P. Converging High-Level Coupled-Cluster Energetics by Monte Carlo Sampling and Moment Expansions. *Phys. Rev. Lett.* **2017**, *119*, 223003, DOI: 10.1103/PhysRevLett.119.223003.
- (105) Gururangan, K.; Deustua, J. E.; Shen, J.; Piecuch, P. High-Level Coupled-Cluster Energetics by Merging Moment Expansions with Selected Configuration Interaction. *J. Chem. Phys.* **2021**, *155*, 174114, DOI: 10.1063/5.0064400.
- (106) Pulay, P. Convergence Acceleration of Iterative Sequences. The Case of SCF Iteration. *Chem. Phys. Lett.* **1980**, *73*, 393–398, DOI: 10.1016/0009-2614(80)80396-4.
- (107) Pulay, P. Improved SCF Convergence Acceleration. *J. Comput. Chem.* **1982**, *3*, 556–560, DOI: 10.1002/jcc.540030413.
- (108) Scuseria, G. E.; Lee, T. J.; Schaefer III, H. F. Accelerating the Convergence of the Coupled-Cluster Approach. *Chem. Phys. Lett.* **1986**, *130*, 236–239, DOI: 10.1016/0009-2614(86)80461-4.
- (109) Nooijen, M. Can the Eigenstates of a Many-Body Hamiltonian Be Represented Exactly Using a General Two-Body Cluster Expansion? *Phys. Rev. Lett.* **2000**, *84*, 2108–2111, DOI: 10.1103/PhysRevLett.84.2108.
- (110) Nakatsuji, H. Structure of the Exact Wave Function. *J. Chem. Phys.* **2000**, *113*, 2949–2956, DOI: 10.1063/1.1287275.
- (111) Stair, N. H.; Evangelista, F. A. QFort: An Efficient State-Vector Emulator and Quantum Algorithms Library for Molecular Electronic Structure. *J. Chem. Theory Comput.* **2022**, *18*, 1555–1568, DOI: 10.1021/acs.jctc.1c01155.
- (112) Smith, D. G. A.; Burns, L. A.; Simmonett, A. C.; Parrish, R. M.; Schieber, M. C.; Galvelis, R.; Kraus, P.; Kruse, H.; Remigio, R. D.; Alenaizan, A. et al. PSI4 1.4: Open-Source Software for High-Throughput Quantum Chemistry. *J. Chem. Phys.* **2020**, *152*, 184108, DOI: 10.1063/5.0006002.
- (113) Kowalski, K.; Piecuch, P. New Coupled-Cluster Methods with Singles, Doubles, and Noniterative Triples for High Accuracy Calculations of Excited Electronic States. *J. Chem. Phys.* **2004**, *120*, 1715–1738, DOI: 10.1063/1.1632474.
- (114) Lutz, J. J.; Piecuch, P. Performance of the Completely Renormalized Equation-of-Motion Coupled-Cluster Method in Calculations of Excited-State Potential Cuts of Water. *Comput. Theor. Chem.* **2014**, *1040–1041*, 20–34, DOI: 10.1016/j.comptc.2014.05.008.
- (115) Piecuch, P.; Hansen, J. A.; Ajala, A. O. Benchmarking the Completely Renormalised Equation-of-Motion Coupled-Cluster Approaches for Vertical Excitation Energies. *Mol. Phys.* **2015**, *113*, 3085–3127, DOI: 10.1080/00268976.2015.1076901.
- (116) Włoch, M.; Gour, J. R.; Kowalski, K.; Piecuch, P. Extension of Renormalized Coupled-Cluster Methods including Triple Excitations to Excited Electronic States of Open-Shell Molecules. *J. Chem. Phys.* **2005**, *122*, 214107, DOI: 10.1063/1.1924596.
- (117) Fradelos, G.; Lutz, J. J.; Wesolowski, T. A.; Piecuch, P. Embedding vs Supermolecular Strategies in Evaluating the Hydrogen-Bonding-Induced Shifts of Excitation Energies. *J. Chem. Theory Comput.* **2011**, *7*, 1647–1666, DOI: 10.1021/ct200101x.

- (118) Yuwono, S. H.; Chakraborty, A.; Deustua, J. E.; Shen, J.; Piecuch, P. Accelerating Convergence of Equation-of-Motion Coupled-Cluster Computations using the Semi-Stochastic CC($P;Q$) Formalism. *Mol. Phys.* **2020**, *118*, e1817592, DOI: 10.1080/00268976.2020.1817592.

Supporting Information:

Unitary Coupled Cluster: Seizing the Quantum Moment

Ilias Magoulas* and Francesco A. Evangelista*

*Department of Chemistry and Cherry Emerson Center for Scientific Computation,
Emory University, Atlanta, Georgia 30322, USA*

E-mail: ilias.magoulas@emory.edu; francesco.evangelista@emory.edu

This Supporting Information document is organized as follows. In Section S1 we provide the proof and underlying conditions for the size-consistency of the non-iterative energy corrections, derived from the formalism of the method of moments of coupled-cluster (MMCC) equations, considered in the main text. Section S2 contains, in a graphical form, additional numerical results.

The numerical data generated in this study can be found in the Excel file that forms part of the present Supporting Information.

S1 Method of Moments of Coupled-Cluster Equations and Unitary Coupled Cluster: Size Consistency

Here, we provide a mathematical proof of the size consistency of the MMUCC formulas considered in the main text, along with the associated necessary and sufficient conditions.

We begin our analysis by examining the isolated systems A and B , characterized by the H_A and H_B Hamiltonians, respectively. The Schrödinger equations for the ground electronic states of each of the two systems read

$$H_A |\Psi_{0,A}\rangle = E_{0,A} |\Psi_{0,A}\rangle \tag{S1}$$

and

$$H_B |\Psi_{0,B}\rangle = E_{0,B} |\Psi_{0,B}\rangle. \tag{S2}$$

The exact $|\Psi_{0,A}\rangle$ and $|\Psi_{0,B}\rangle$ electronic states can be expressed in terms of the following unitary parametrizations:

$$|\Psi_{0,A}\rangle = U_A |\Phi_A\rangle \tag{S3}$$

and

$$|\Psi_{0,B}\rangle = U_B |\Phi_B\rangle, \tag{S4}$$

with U_A and U_B representing products of elementary unitary excitation operators, and $|\Phi_A\rangle$ and $|\Phi_B\rangle$ denoting the reference Slater determinants of systems A and B , respectively. The corresponding sets of all excited determinants afforded by the respective one-electron bases are denoted $\{|\Phi_{k,A}\rangle\}$ for system A and $\{|\Phi_{k,B}\rangle\}$ in the case of system B . Without loss of generality, we assume the use of canonical Hartree–Fock orbitals. The many-electron Hilbert space of system A , \mathcal{H}_A , can be partitioned as $\mathcal{H}_A = \mathcal{H}_{0,A} \oplus \mathcal{H}_{K,A}$, where $\mathcal{H}_{0,A} = \text{span}(|\Phi_A\rangle)$ and $\mathcal{H}_{K,A} = \text{span}(\{|\Phi_{k,A}\rangle\})$. Similar definitions apply in the case of system B . The fact that $|\Psi_{0,A}\rangle$ and $|\Psi_{0,B}\rangle$ are exact implies the following residual conditions:

$$\langle \Phi_{k,A} | \bar{H}_A | \Phi_A \rangle = 0, \forall |\Phi_{k,A}\rangle \in \mathcal{H}_{K,A} \quad (\text{S5})$$

and

$$\langle \Phi_{k,B} | \bar{H}_B | \Phi_B \rangle = 0, \forall |\Phi_{k,B}\rangle \in \mathcal{H}_{K,B}, \quad (\text{S6})$$

where $\bar{H}_A = U_A^\dagger H_A U_A$ and $\bar{H}_B = U_B^\dagger H_B U_B$ are the pertinent similarity transformed Hamiltonians.

Subsequently, we turn our attention to an approximate description of the isolated systems A and B . In this case, the $U_A^{(P_A)}$ and $U_B^{(P_B)}$ unitaries that define the $|\Psi_{0,A}^{(P_A)}\rangle$ and $|\Psi_{0,B}^{(P_B)}\rangle$ ansätze,

$$|\Psi_{0,A}^{(P_A)}\rangle = U_A^{(P_A)} |\Phi_A\rangle \quad (\text{S7})$$

and

$$|\Psi_{0,B}^{(P_B)}\rangle = U_B^{(P_B)} |\Phi_B\rangle, \quad (\text{S8})$$

contain fewer parameters than the dimensions of the $\mathcal{H}_{K,A}$ and $\mathcal{H}_{K,B}$ spaces, respectively. Consequently, the residual conditions can only be satisfied in the $\mathcal{H}_{P,A} \subset \mathcal{H}_{K,A}$ and $\mathcal{H}_{P,B} \subset \mathcal{H}_{K,B}$ subspaces corresponding to the excitation operators appearing in the $U_A^{(P_A)}$ and $U_B^{(P_B)}$ unitaries:

$$\langle \Phi_{p,A} | \bar{H}^{(P_A)} | \Phi_A \rangle = 0, \forall |\Phi_{p,A}\rangle \in \mathcal{H}_{P,A} \quad (\text{S9})$$

and

$$\langle \Phi_{p,B} | \bar{H}^{(P_B)} | \Phi_B \rangle = 0, \forall |\Phi_{p,B}\rangle \in \mathcal{H}_{P,B}. \quad (\text{S10})$$

The $\mathcal{H}_{Q,A} \equiv \mathcal{H}_{K,A} \ominus \mathcal{H}_{P,A}$ and $\mathcal{H}_{Q,B} \equiv \mathcal{H}_{K,B} \ominus \mathcal{H}_{P,B}$ subspaces are spanned by the excited Slater determinants $\{|\Phi_{q,A}\rangle\}$ and $\{|\Phi_{q,B}\rangle\}$, respectively, that do not satisfy the pertinent residual conditions.

Next we consider the electronic structure of the supersystem AB , comprised of the non-interacting systems A and B . Since there is no coupling between the two systems, the Hamiltonian of supersystem AB is

$$H_{AB} = H_A \otimes \mathbf{1}_B + \mathbf{1}_A \otimes H_B \equiv H_A + H_B, \quad (\text{S11})$$

with $\mathbf{1}_A$ and $\mathbf{1}_B$ denoting the identity operators on the \mathcal{H}_A and \mathcal{H}_B many-electron Hilbert spaces, respectively. Due to the fact that factorized UCC ansätze are not orbital-invariant, the choice of orbitals is crucial for achieving size consistency. To that end, we consider a localized orbital basis, comprised of the canonical Hartree–Fock orbitals of systems A and B . The use of a localized basis and the fact that systems A and B do not interact imply that the unitaries defining the exact and approximate ansätze of supersystem AB will only involve localized excitations, i.e.,

$$|\Psi_{0,AB}\rangle = U_{AB} |\Phi_{AB}\rangle = U_A U_B |\Phi_{AB}\rangle \quad (\text{S12})$$

and

$$|\Psi_{0,AB}^{(P_A, P_B)}\rangle = U_{AB}^{(P_A, P_B)} |\Phi_{AB}\rangle = U_A^{(P_A)} U_B^{(P_B)} |\Phi_{AB}\rangle, \quad (\text{S13})$$

with $|\Phi_{AB}\rangle$ being the reference determinant of the supersystem AB . Furthermore, the operators H_A , U_A , and $U_A^{(P_A)}$ and H_B , U_B , and $U_B^{(P_B)}$ pairwise commute since they are acting on different spaces. Note that to ensure the proper multiplicative separability of the wavefunction and additivity of the energy, the ordering of the elementary anti-Hermitian excitation

operators defining the U_A , U_B , $U_A^{(P_A)}$, and $U_B^{(P_B)}$ unitaries needs to be preserved between the computations for the isolated systems A and B and the non-interacting supersystem AB . Assuming that $|\Phi_{AB}\rangle$ is separable, namely,

$$|\Phi_{AB}\rangle = |\Phi_A\rangle \otimes |\Phi_B\rangle \equiv |\Phi_A\rangle |\Phi_B\rangle, \quad (\text{S14})$$

we arrive at the separability of the underlying $|\Psi_{0,AB}\rangle$ and $|\Psi_{0,AB}^{(P_A, P_B)}\rangle$ states:

$$|\Psi_{0,AB}\rangle = U_A |\Phi_A\rangle U_B |\Phi_B\rangle = |\Psi_{0,A}\rangle |\Psi_{0,B}\rangle \quad (\text{S15})$$

and

$$|\Psi_{0,AB}^{(P_A, P_B)}\rangle = U_A^{(P_A)} |\Phi_A\rangle U_B^{(P_B)} |\Phi_B\rangle = |\Psi_{0,A}^{(P_A)}\rangle |\Psi_{0,B}^{(P_B)}\rangle. \quad (\text{S16})$$

First, we consider the δ_{II} MMCC correction, eq (16) of the main text, since the proof is somewhat more involved. It is straightforward to show that in the case of the non-interacting supersystem AB , $\delta_{\text{II},0}^{(P_A, P_B)}$ becomes

$$\begin{aligned} \delta_{\text{II},0}^{(P_A, P_B)} = & \sum_{|\Phi_{q,A}\rangle \in \mathcal{H}_{Q,A}} \frac{\langle \Psi_0 | U^{(P_A, P_B)} |\Phi_{q,A}\rangle |\Phi_B\rangle \langle \Phi_{q,A} | \langle \Phi_B | \bar{H}^{(P_A, P_B)} |\Phi_A\rangle |\Phi_B\rangle}{\langle \Psi_0 | \Psi_0^{(P_A, P_B)} \rangle} + \\ & \sum_{|\Phi_{q,B}\rangle \in \mathcal{H}_{Q,B}} \frac{\langle \Psi_0 | U^{(P_A, P_B)} |\Phi_A\rangle |\Phi_{q,B}\rangle \langle \Phi_A | \langle \Phi_{q,B} | \bar{H}^{(P_A, P_B)} |\Phi_A\rangle |\Phi_B\rangle}{\langle \Psi_0 | \Psi_0^{(P_A, P_B)} \rangle} + \\ & \sum_{\substack{|\Phi_{q,A}\rangle \in \mathcal{H}_{Q,A} \\ |\Phi_{q,B}\rangle \in \mathcal{H}_{Q,B}}} \frac{\langle \Psi_0 | U^{(P_A, P_B)} |\Phi_{q,A}\rangle |\Phi_{q,B}\rangle \langle \Phi_{q,A} | \langle \Phi_{q,B} | \bar{H}^{(P_A, P_B)} |\Phi_A\rangle |\Phi_B\rangle}{\langle \Psi_0 | \Psi_0^{(P_A, P_B)} \rangle} \end{aligned} \quad (\text{S17})$$

The above expression can be simplified since

$$\begin{aligned} \langle \Phi_{q,A} | \langle \Phi_{q,B} | \bar{H}^{(P_A, P_B)} |\Phi_A\rangle |\Phi_B\rangle &= \langle \Phi_{q,A} | \langle \Phi_{q,B} | (\bar{H}_A^{(P_A)} + \bar{H}_B^{(P_B)}) |\Phi_A\rangle |\Phi_B\rangle \\ &= \langle \Phi_{q,A} | \bar{H}_A^{(P_A)} |\Phi_A\rangle \langle \Phi_{q,B} | \Phi_B\rangle + \langle \Phi_{q,B} | \bar{H}_B^{(P_B)} |\Phi_B\rangle \langle \Phi_{q,A} | \Phi_A\rangle \\ &= 0, \end{aligned} \quad (\text{S18})$$

where in the last step we used the fact that Slater determinants are orthonormal. Therefore, eq (S17) reduces to

$$\delta_{\text{II},0}^{(P_A,P_B)} = \sum_{|\Phi_{q,A}\rangle \in \mathcal{H}_{Q,A}} \frac{\langle \Psi_0 | U^{(P_A,P_B)} | \Phi_{q,A} \rangle | \Phi_B \rangle \langle \Phi_{q,A} | \langle \Phi_B | \bar{H}^{(P_A,P_B)} | \Phi_A \rangle | \Phi_B \rangle}{\langle \Psi_0 | \Psi_0^{(P_A,P_B)} \rangle} + \sum_{|\Phi_{q,B}\rangle \in \mathcal{H}_{Q,B}} \frac{\langle \Psi_0 | U^{(P_A,P_B)} | \Phi_A \rangle | \Phi_{q,B} \rangle \langle \Phi_A | \langle \Phi_{q,B} | \bar{H}^{(P_A,P_B)} | \Phi_A \rangle | \Phi_B \rangle}{\langle \Psi_0 | \Psi_0^{(P_A,P_B)} \rangle} . \quad (\text{S19})$$

Before we are able to proceed any further, we need to evaluate the various quantities appearing in eq (S19). Starting with the denominator that is common in both terms, it is fairly straightforward to show that it factorizes as follows:

$$\langle \Psi_0 | \Psi_0^{(P_A,P_B)} \rangle = \langle \Psi_{0,A} | \Psi_{0,A}^{(P_A)} \rangle \langle \Psi_{0,B} | \Psi_{0,B}^{(P_B)} \rangle . \quad (\text{S20})$$

Focusing on the first term, we have that

$$\begin{aligned} \langle \Psi_0 | U^{(P_A,P_B)} | \Phi_{q,A} \rangle | \Phi_B \rangle &= \langle \Phi_A | \langle \Phi_B | U_A^\dagger U_B^\dagger U_A^{(P_A)} U_B^{(P_B)} | \Phi_{q,A} \rangle | \Phi_B \rangle \\ &= \langle \Phi_A | U_A^\dagger U_A^{(P_A)} | \Phi_{q,A} \rangle \langle \Phi_B | U_B^\dagger U_B^{(P_B)} | \Phi_B \rangle \\ &= \langle \Psi_{0,A} | U_A^{(P_A)} | \Phi_{q,A} \rangle \langle \Psi_{0,B} | \Psi_{0,B}^{(P_B)} \rangle \end{aligned} \quad (\text{S21})$$

and

$$\begin{aligned} \langle \Phi_{q,A} | \langle \Phi_B | \bar{H}^{(P_A,P_B)} | \Phi_A \rangle | \Phi_B \rangle &= \langle \Phi_{q,A} | \langle \Phi_B | (\bar{H}_A^{(P_A)} + \bar{H}_B^{(P_B)}) | \Phi_A \rangle | \Phi_B \rangle \\ &= \langle \Phi_{q,A} | \bar{H}_A^{(P_A)} | \Phi_A \rangle \langle \Phi_B | \Phi_B \rangle + \langle \Phi_B | \bar{H}_B^{(P_B)} | \Phi_B \rangle \langle \Phi_{q,A} | \Phi_A \rangle \\ &= \langle \Phi_{q,A} | \bar{H}_A^{(P_A)} | \Phi_A \rangle . \end{aligned} \quad (\text{S22})$$

Similar expressions can be derived in the case of the second term appearing in eq (S19).

We are now in a position to derive the final expression for the non-iterative moment

correction for the supersystem. Using the above information, eq (S19) yields

$$\begin{aligned}
\delta_{\text{II},0}^{(P_A,P_B)} &= \sum_{|\Phi_{q,A}\rangle \in \mathcal{H}_{Q,A}} \frac{\langle \Psi_{0,A} | U_A^{(P_A)} | \Phi_{q,A} \rangle \langle \Psi_{0,B} | \Psi_{0,B}^{(P_B)} \rangle \langle \Phi_{q,A} | \bar{H}_A^{(P_A)} | \Phi_A \rangle}{\langle \Psi_{0,A} | \Psi_{0,A}^{(P_A)} \rangle \langle \Psi_{0,B} | \Psi_{0,B}^{(P_B)} \rangle} + \\
&\quad \sum_{|\Phi_{q,B}\rangle \in \mathcal{H}_{Q,B}} \frac{\langle \Psi_{0,B} | U_B^{(P_B)} | \Phi_{q,B} \rangle \langle \Psi_{0,A} | \Psi_{0,A}^{(P_A)} \rangle \langle \Phi_{q,B} | \bar{H}_B^{(P_B)} | \Phi_B \rangle}{\langle \Psi_{0,A} | \Psi_{0,A}^{(P_A)} \rangle \langle \Psi_{0,B} | \Psi_{0,B}^{(P_B)} \rangle} \\
&= \sum_{|\Phi_{q,A}\rangle \in \mathcal{H}_{Q,A}} \frac{\langle \Psi_{0,A} | U_A^{(P_A)} | \Phi_{q,A} \rangle \langle \Phi_{q,A} | \bar{H}_A^{(P_A)} | \Phi_A \rangle}{\langle \Psi_{0,A} | \Psi_{0,A}^{(P_A)} \rangle} + \\
&\quad \sum_{|\Phi_{q,B}\rangle \in \mathcal{H}_{Q,B}} \frac{\langle \Psi_{0,B} | U_B^{(P_B)} | \Phi_{q,B} \rangle \langle \Phi_{q,B} | \bar{H}_B^{(P_B)} | \Phi_B \rangle}{\langle \Psi_{0,B} | \Psi_{0,B}^{(P_B)} \rangle} \\
&= \delta_{\text{II},0}^{(P_A)} + \delta_{\text{II},0}^{(P_B)}.
\end{aligned} \tag{S23}$$

Therefore, we proved that the MMCC-type correction defined by eq (16) of the main text is size-consistent, provided that the following conditions are satisfied:

1. Use of orbitals localized on the individual fragments.
2. Separability of the underlying reference state.
3. The ordering of the elementary unitary excitation operators needs to be identical in the isolated fragments and the supersystem.

The proof that the δ_{Ia} and δ_{Ic} non-iterative MMCC-type corrections, given by eqs (9) and (15), respectively, of the main text, are also size-consistent follows the same steps as above, depending on the same conditions as well.

S2 Additional Numerical Results

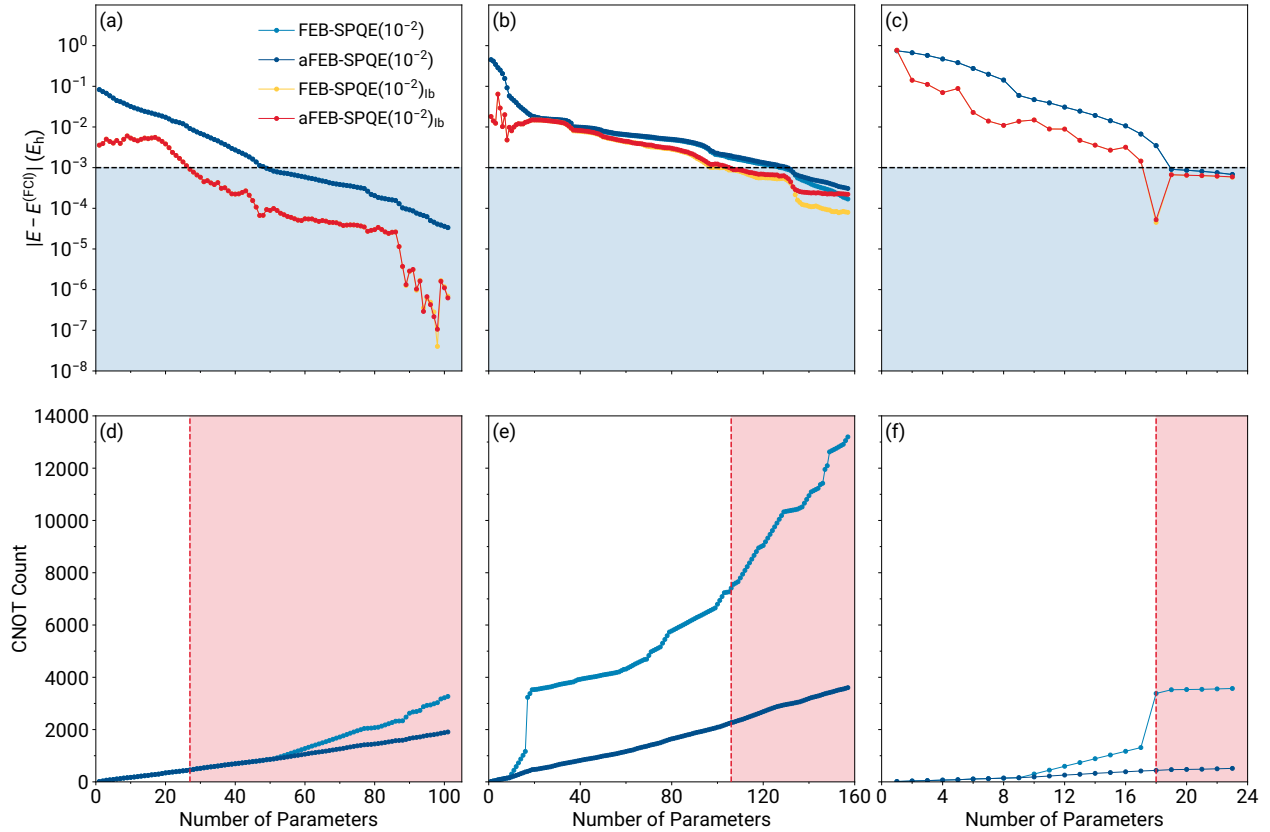


Figure S1: Errors relative to FCI [(a)–(c)] and CNOT gate counts [(d)–(f)] characterizing the aFEB-SPQE simulations of the symmetric dissociation of the H_6 /STO-6G linear chain at three representative distances between neighboring H atoms, including $R_{H-H} = 1.0 \text{ \AA}$ [(a) and (d)], $R_{H-H} = 2.0 \text{ \AA}$ [(b) and (e)], and $R_{H-H} = 3.0 \text{ \AA}$ [(c) and (f)]. The blue-shaded area in the top-row panels indicates results within chemical accuracy ($1 mE_h$) from FCI. The red-shaded area in the bottom-row panels denotes the CNOT counts of the underlying aFEB-SPQE quantum circuits for which the aFEB-SPQE_{lb} energetics are within chemical accuracy. To facilitate comparisons, the corresponding FEB-SPQE results are also included.

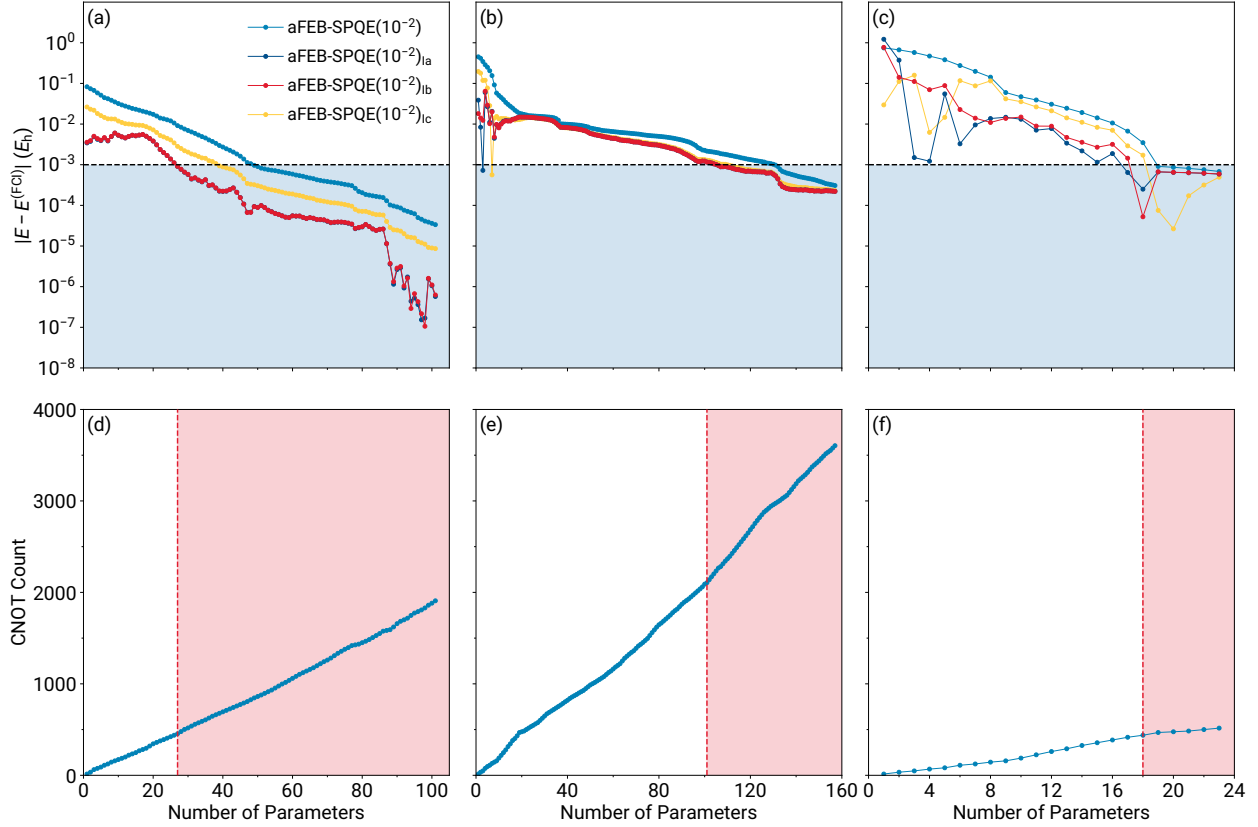


Figure S2: Errors relative to FCI [(a)–(c)] and CNOT gate counts [(d)–(f)] characterizing the aFEB-SPQE simulations of the symmetric dissociation of the $H_6/STO-6G$ linear chain at three representative distances between neighboring H atoms, including $R_{H-H} = 1.0 \text{ \AA}$ [(a) and (d)], $R_{H-H} = 2.0 \text{ \AA}$ [(b) and (e)], and $R_{H-H} = 3.0 \text{ \AA}$ [(c) and (f)]. The blue-shaded area in the top-row panels indicates results within chemical accuracy ($1 mE_h$) from FCI. The red-shaded area in the bottom-row panels denotes the CNOT counts of the underlying aFEB-SPQE quantum circuits for which the aFEB-SPQE_{1b} energies are within chemical accuracy.

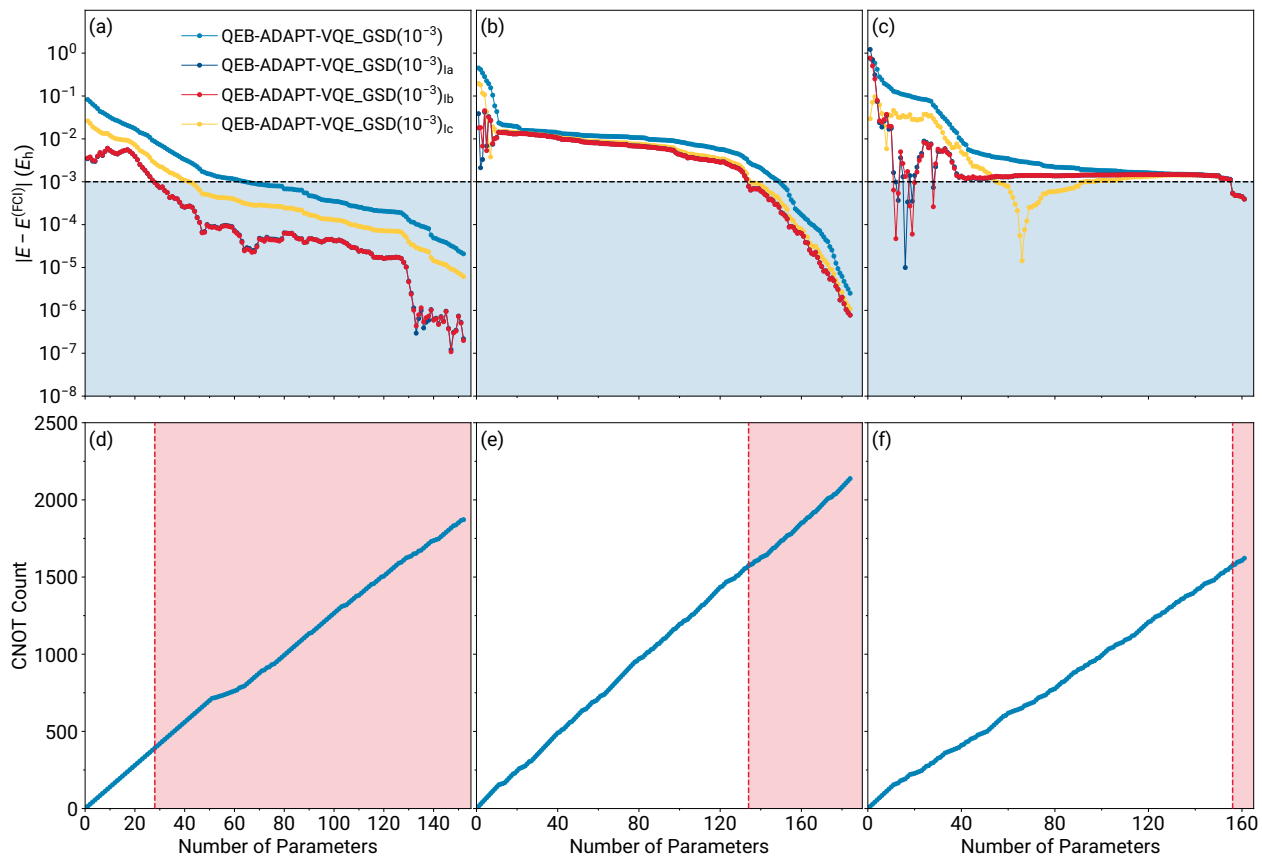


Figure S3: Errors relative to FCI [(a)–(c)] and CNOT gate counts [(d)–(f)] characterizing the QEB-ADAPT-VQE simulations of the symmetric dissociation of the $\text{H}_6/\text{STO-6G}$ linear chain at three representative distances between neighboring H atoms, including $R_{\text{H-H}} = 1.0 \text{ \AA}$ [(a) and (d)], $R_{\text{H-H}} = 2.0 \text{ \AA}$ [(b) and (e)], and $R_{\text{H-H}} = 3.0 \text{ \AA}$ [(c) and (f)]. The blue-shaded area in the top-row panels indicates results within chemical accuracy ($1 mE_h$) from FCI. The red-shaded area in the bottom-row panels denotes the CNOT counts of the underlying QEB-ADAPT-VQE quantum circuits for which the QEB-ADAPT-VQE_{1b} energies are within chemical accuracy.